



REVIEW

# Energy Absorption Characteristics of Fused Deposition Modeling 3D Printed Auxetic Re-entrant Structures: A Review

*Niranjan Kumar Choudhry, Biranchi Panda, and Uday Shanker Dixit*

Submitted: 1 October 2022 / Revised: 25 March 2023 / Accepted: 4 April 2023 / Published online: 3 May 2023

This article summarizes the latest advances in manufacturing of negative Poisson's ratio materials, so-called auxetic materials, their structural mechanics and energy absorption capabilities. Diverse examples of application of these materials have been provided. Due to their excellent energy absorption capability and functional performance, these materials have generated significant interest in several applications including medical implants, automobile and sport items. It is possible to tailor their macroscopic properties by tuning the architectural features at the meso-scale, thanks to developments in 3D printing technologies. The current research is dominated by auxetic materials with periodic or ordered microstructures. The main focus of this review paper is to discuss the progress in energy absorption performance of re-entrant structures manufactured by fused deposition modeling 3D printing process. After highlighting the knowledge gaps in existing literature, this review provides an outlook on the possible future research. It is expected to gain new insights into the design and modeling of re-entrant structures for different industrial applications.

**Keywords** 3D printing, auxetics, cellular structures, energy absorption, negative Poisson's ratio, re-entrant lattice structure

## 1. Introduction

Auxetic structures exhibit exceptional properties such as high specific stiffness, strength and energy absorption capability in comparison with conventional materials due to their unique architectural design (Ref 1, 2). Inspiration for design of such structures often comes from naturally occurring materials such as cork and sponge; their design can be parametrically tailored to suit various engineering applications (Ref 3, 4). In recent years, due to advancements in 3D printing processes, extensive studies have been carried out on auxetic structures for different applications as depicted pictorially in Fig. 1. Auxetic materials or structures behave differently than conventional materials, i.e., they shrink during compression and expand during tension (Fig. 2). Evans (Ref 5) used the term “auxetics” first time for structures or materials showing a negative Poisson's ratio (NPR). As per (Ref 6), Almgren first introduced a new type of auxetic structure called “two-dimensional re-entrant honeycomb structure” in 1985 by introducing a strut in the honeycomb structure. This structure exhibits a negative

Poisson's ratio under compression. Its performance can be varied by choosing a suitable material and structural design.

Figure 3 shows the publication trend of re-entrant auxetic structures collected from the year 2000 to 2023. This trend is based on Scopus search engine accessed on March 19, 2023, by using the keywords “re-entrant structure, arrowed structure, star structure, hybrid re-entrant structure and graded re-entrant structure” and including the articles under “Engineering” and “Multidisciplinary.” If other categories are included, the number of published articles increases approximately twofold. Web of Science search engine also provides similar trend. It can be seen that initially (up to 2015) only a few articles were published, but thereafter there is an exponential growth in the number of publications. This indicates the increased interest of researchers in auxetic re-entrant structures and their applications. A good number of review papers have been published on auxetic mechanical metamaterials, but there is hardly a comprehensive review article on 3D printed re-entrant auxetic structures for energy absorption application. This review article fills up this gap in the literature.

This paper reviews the latest development of two-dimensional (2D) auxetic re-entrant structures for energy absorption (under quasi-static loading) for various industrial applications. Different variants of re-entrant structures such as regular re-entrant honeycomb, hybrid re-entrant, graded re-entrant and sandwich structures using these re-entrant structures as the core materials are reviewed. The deformation mechanisms of these re-entrant structures, which lead to higher energy absorption properties, are also studied in this paper. The aim of the review is to understand the ongoing development in re-entrant structures for achieving higher energy absorption and their key applications, while highlighting the challenges of manufacturing by the extrusion-based 3D printing process. The review combines engineering design and mechanistic under-

**Niranjan Kumar Choudhry, Biranchi Panda, and Uday Shanker Dixit**, Department of Mechanical Engineering, Indian Institute of Technology Guwahati, Guwahati, India. Contact e-mail: pandabiranchi@iitg.ac.in.

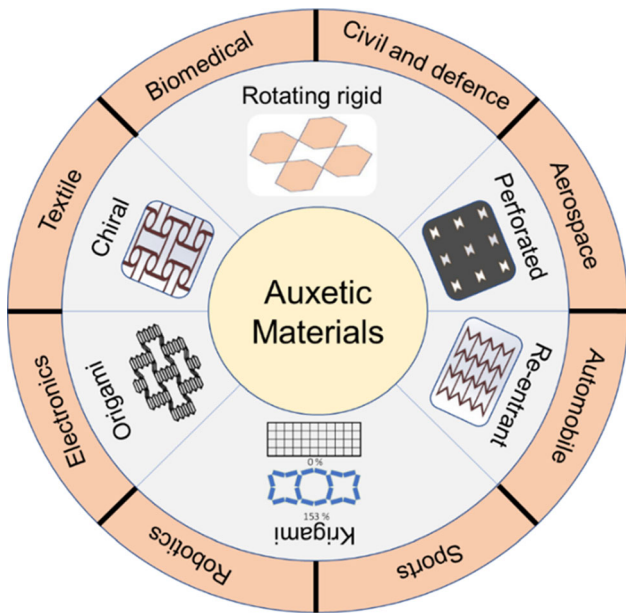


Fig. 1 Classification and applications of auxetic structures

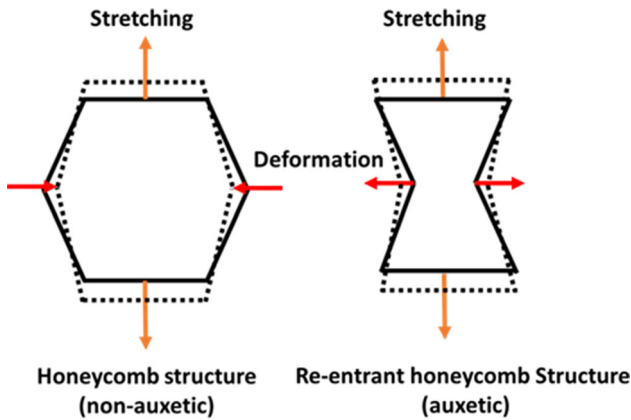


Fig. 2 Effect of loading on auxetic and non-auxetic structures

standing for fabrication of auxetic materials. It also highlights what remains to be improved and where research is urgently needed for future development.

## 2. Research on Energy Absorption of Re-entrant Structures

In this section, particular attention is paid to in-plane energy absorption behavior of fused deposition modeling printed re-entrant structures. Basically, re-entrant structures are closed polygons that have at least one negative angle (internal angle more than  $180^\circ$ ). A progressive study on lattice design has been made to understand how the evolution in design takes place over a period of time (Fig. 4a). The purpose of evolution in design is to improve the re-entrant lattice structure's energy absorption performance. A detailed study has been made in the following subsection. The scope of the review article is limited to quasi-static loading conditions (strain rates in the range of  $10^{-5} \sim 1 \text{ s}^{-1}$ ).

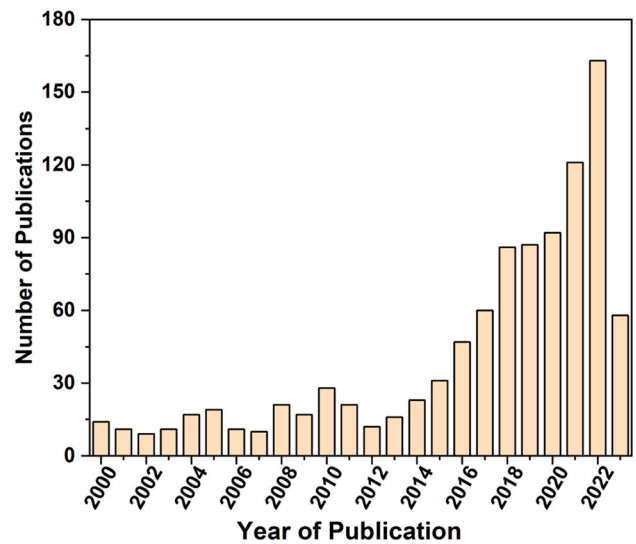


Fig. 3 Publication trends of re-entrant auxetic structures from 2000 to 2023

The energy absorption capacity (in  $\text{MJ/m}^3$ ) of any lattice structure is determined by the area under the stress–strain curve starting from the beginning and covering up to the onset of densification. There are three different ways to identify the onset of densification ( $\epsilon_D$ ) (Ref 7) as presented in Fig. 4(b). The first method is used when there is a sharp rise in stress in stress–strain response, while the second and third methods are used when there is no such sharp rise in stress in stress–strain response.

In the first method, the onset of densification is identified by locating a sharp rise in stress value, while in the second method, a line parallel to the strain axis is drawn from the peak stress ( $\sigma_p$ ) which intersects the stress–strain curve and the corresponding intersecting strain is identified as the onset of densification. In the third method (efficiency method), energy absorption efficiency  $\eta$  is plotted against the strain, and the corresponding strain having the highest efficiency is identified as the onset of densification. The efficiency as a function of strain is calculated as

$$\eta = \frac{E_{ab}}{\sigma_{\max}}, \quad (\text{Eq 1})$$

where  $\sigma_{\max}$  is the maximum stress up to strain  $\epsilon$  and energy absorbed is given by

$$E_{ab} = \int_0^\epsilon \sigma d\epsilon. \quad (\text{Eq 2})$$

The energy absorption characteristics of auxetic structure mainly depend on its plateau region, which is the area under the stress–strain curve starting from the yield point to the onset of densification; the larger the plateau area the more will be energy absorption capacity (Ref 8). The energy absorption performance is correlated with their specific energy absorption (SEA); the greater the specific energy absorption, the better the lattice structure. Specific energy absorption is calculated by dividing  $E_{ab}$  with density of the lattice structure.

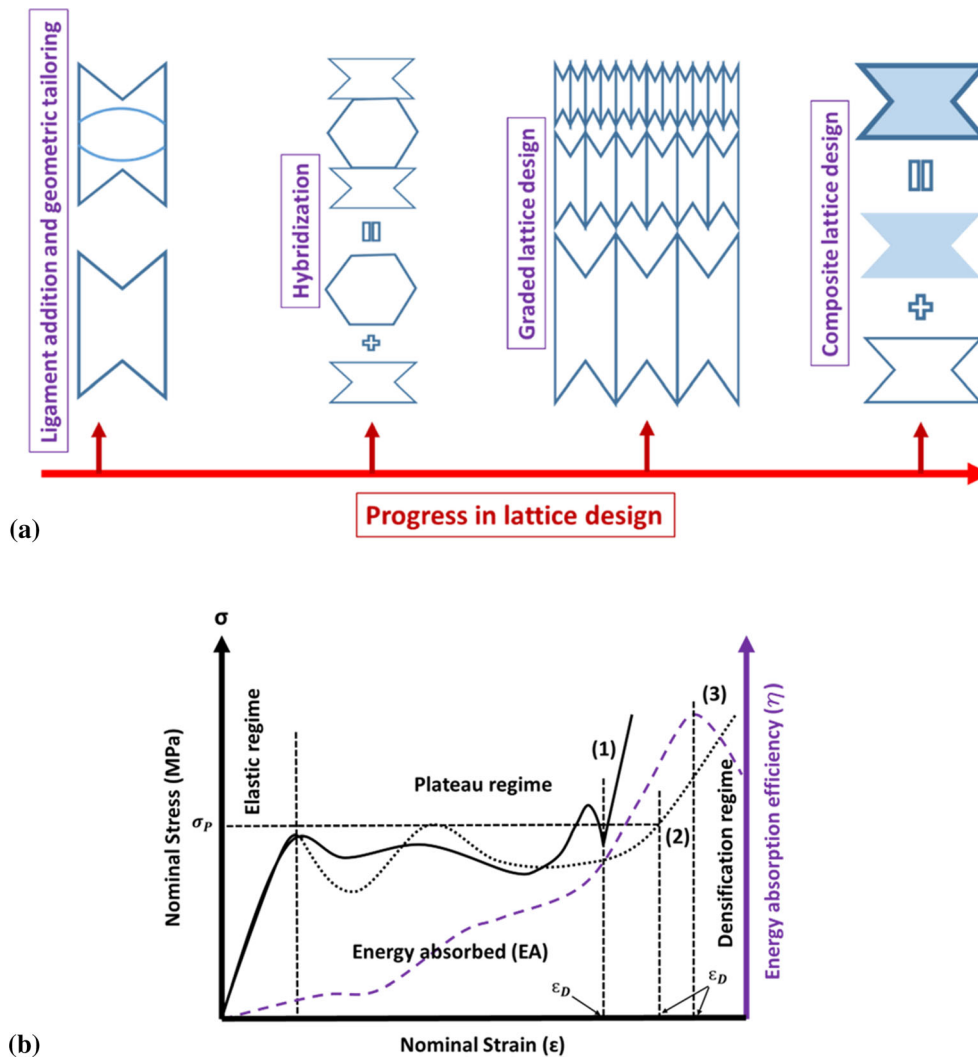


**Fig. 4** Schematic presentation of (a) evolution in lattice design of re-entrant structure for improvement in energy absorption performance and (b) different methods used to identify the onset of densification ( $\epsilon_D$ ) strain and their corresponding energy absorption performance

## 2.1 Regular Re-entrant Structure

Many researchers have explored the 3D printed re-entrant structures and revealed their mechanical properties due to their negative Poisson's ratio property (Ref 1, 9-12). Figure 5(a) shows a typical re-entrant structure comprising straight and inclined struts. As a re-entrant structure shows anisotropic behavior, the in-plane crushing performance of the re-entrant structure can be studied in two different loading conditions—(1) loading perpendicular to the straight strut and (2) loading parallel to the straight strut (Fig. 5a). For all the cases deformation mechanism is the same for the FDM printed re-entrant lattices, but the deformation patterns formed are different, causing the variation in the crushing response (mechanical properties) of the re-entrant structure.

**2.1.1 Deformation Mechanisms.** The failure of re-entrant structure follows bending-dominated mechanism. Deformation mechanism unfolds behavior of different ligaments when subjected to the compressive loading. The structures exhibit the elastic-plastic collapse behavior in three distinct stages—elastic regime, plateau regime and densification regime (Ref 3, 13) at the macro-scale as shown in Fig. 5(b), (c) and (d).

The elastic regime is the first stage where the structures undergo linear-elastic deformation. During the linear elastic compression phase, inclined members experience axial, bending and shear loading (Ref 3, 14). Further, as compression continues, the stress in the inclined member reaches to its critical stress, and the cell collapses near the joint due to the formation of a plastic hinge (Ref 15, 16). Elastic regime is mostly governed by the bending performance of the inclined members.

In the second stage, viz. plateau regime (post-yielding), the structure starts deforming plastically resulting in a long plateau region. In this stage, the strut behaves like a perfectly rigid plastic material, and the cell collapses either due to plastic hinge formation or due to the buckling, in case the load in the member exceeds Euler buckling load. Once all the cells present in a row of the structure collapse, the deformation waves move to the other row. This continues till whole structure collapses. During the plateau regime, stress peaks and valleys are formed. Peaks are formed when cells of the deforming row resist the loading before the start of collapse, while valleys are formed when cells of the deforming rows completely collapse. Finally, in the densification regime, when all the rows of the structure collapse, there is a sharp increase in the stress, which is mainly

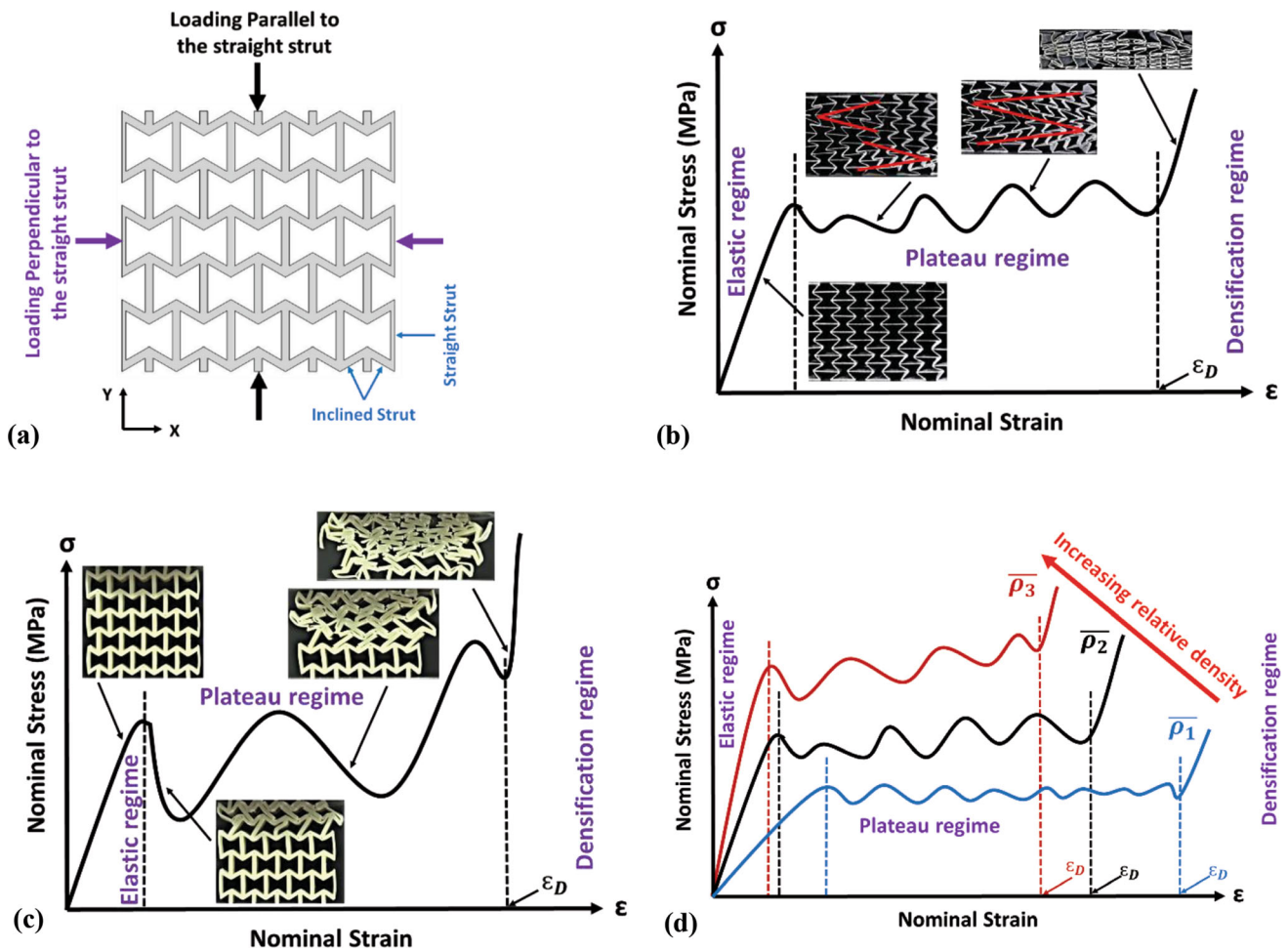


**Fig. 5** Quasi-static compression response of auxetic structure: (a) re-entrant honeycomb structure, (b) representative stress–strain response of re-entrant structure when loaded perpendicular and (c) parallel to the straight strut, (d) effect of strut wall thickness on the stress–strain response

due to the compaction of the cells (as within the compaction phase the performance is determined by the matrix material and not by the structure (Ref 17) and the stiffness of the matrix material is higher than the structure). In the compaction phase, the stress–strain behavior of the structure depends on the material of the structure (Ref 18).

**2.1.2 Effect of Loading Direction on the Crushing Performance and Deformation Pattern.** There is an effect of loading direction on the crushing performance of lattice structures, especially on the deformation patterns and their mechanical responses. The deformation patterns of the re-entrant structure when loaded perpendicular to the straight strut are shown in Fig. 5(b). In this loading direction, the re-entrant structure shows wider elastic regime with lower yield stress, which is desirable for the packaging industry. Once the structure starts deforming plastically (beginning of plateau regime), the cell wall of the structure shrinks locally and expands at boundaries, forming a double horizontal V-like pattern. This type of pattern resists the formation of peaks and valleys and provides an almost stable or flat plateau region. Further compression causes a change in the deformation pattern. The double horizontal V-type deformation pattern is shifted to a Z-like pattern, and gradually, the structure reaches densification (Fig. 5b) (Ref 19). This type of deformation

pattern gives more stable and longer plateau region with lower plateau stress.

On the other hand, the deformation patterns and mechanical response of the re-entrant structure loaded parallel to the straight strut are quite different. The stress–strain curve of a re-entrant honeycomb structure (RH) under this loading condition is shown in Fig. 5(c). Like perpendicular loading conditions, it also exhibits three distinct deformation stages as reported by many researchers (Ref 15, 20, 21). However, the formation of patterns in the deformation mechanism is different (Ref 22, 23). In the linear elastic stage, cells of the RH structure deformed uniformly throughout the lattice and reached the maximum value. The cell walls which were parallel to the loading direction exhibited their behavior like an end-loaded column and buckled when the load exceeded Euler buckling load, while the other inclined cell walls bent as shown in Fig. 5(c). At the node where three walls meet, deformation was controlled by the rotational stiffness of the node. The inclined walls affected rotational stiffness greatly as they determine the degree of constraint to rotation (Ref 3) and led to buckling and bending of the cell walls. Due to this, moments were generated and responsible for sideways collapse of the cell. The stiffness and yield stress are always greater than those of the perpendicular loading condition.



Once the stress increases to its maximum value, its value drops as the first layer of cell walls collapses. After that, the stress again increases due to the densification of collapsed cells. This cyclic behavior of stress (increasing and decreasing) continues till all the rows collapse, forming peaks and valleys, leading to an unstable plateau region (Fig. 5c). Collapsing of the cell starts from one end of the lattice and propagates toward the other end till it completely collapses. Finally, when all the rows of the structures collapse, densification starts. This type of deformation pattern gives a less stable shorter plateau region with higher yield stress.

**2.1.3 Effect of Wall Thickness on the Crushing Performance of a Re-entrant Structure.** Figure 5(d) shows the effect of strut wall thickness on the stress–strain response of a re-entrant auxetic structure. The increase in relative density is mainly due to increase in the wall thickness of struts; the geometry of the structure remains unchanged. It was found that a thick-walled re-entrant honeycomb structure deformed differently than a thin-walled re-entrant honeycomb structure (Ref 19). As the thickness of the lattice wall increases, there is a sharp increase in the stiffness and yield stress, while the elastic regime reduces.

There is an impact of lattice wall thickness on the plateau regime also. Due to increase in the wall thickness, there is a change in the deformation patterns. For perpendicular loading conditions, it forms a vertical V-like deformation pattern during the early stage of compression as the cell at the top-mid part moves toward the interior-mid portion. As compression continues, cell rupture starts along with cell wall movement, which is responsible for the change of the deformation pattern from vertical V mode to Y mode and finally to X mode. In the case of parallel loading conditions, due to increase in the thickness of cell wall, the distance between the walls reduces leading to early failure (due to early percolation of contacts between cell walls) (Ref 3). This reduces the onset of densification that ultimately reduces the total energy absorption. The thicker wall of the cell results in early densification with higher plateau stress and a reduction in energy absorption capacity. Hence, thicker walls are undesirable.

## 2.2 Evolution in Re-entrant Lattice Structure Design

In recent years, numerous studies have explored re-entrant structures, aiming to improve mechanical properties without much increase in mass. In this section, a detailed study has been presented on the development of lattice design and its impact on mechanical performance. All proposed methods are broadly classified into four groups—ligament addition and geometric tailoring, hybridization, graded lattice design and composite lattice (Fig. 4a).

**2.2.1 Ligament Addition and Geometric Tailoring.** In this method, mechanical performance such as energy absorption and stiffness of the regular re-entrant structure is improved either by geometric tailoring or ligament addition or by combining both. A re-entrant structure with its geometrical parameter is shown in Fig. 6, where  $l$ ,  $h$ ,  $t$  and  $\theta$  represent the length of inclined ligaments, the height of straight ligaments, the thickness of ligaments and the angle between the straight and inclined ligaments, respectively.

In the geometric tailoring method, the structures are developed either by varying the geometric parameters (as shown in Fig. 6) or by introducing lower node connectivity by splitting the ligaments. It has been observed that the key factors for designing the new re-entrant structure by varying the geometric parameters are  $\theta$  and  $h/l$  ratio designated by  $\alpha$ . Figure 7(a) and (b) shows the effect of re-entrant angle  $\theta$  and  $\alpha$  on the normalized Young's modulus. Normalized Young's modulus is the ratio of stiffness of the lattice structure  $E$  to that of base material  $E_s$  (Ref 24). The normalization helps in comparing two designs of different materials. For loading parallel to the straight ligament, the influence of the re-entrant angle (identified by the slope of the curve) on the normalized Young's modulus is higher for a smaller re-entrant angle and it reduces as the re-entrant angle increases; it becomes less effective at high re-entrant angle (Fig. 7a) (Ref 24, 25). For loading perpendicular to the straight ligament, the re-entrant angle has opposite trend for the normalized Young's modulus. For smaller re-entrant angles, it is less dominant and becomes

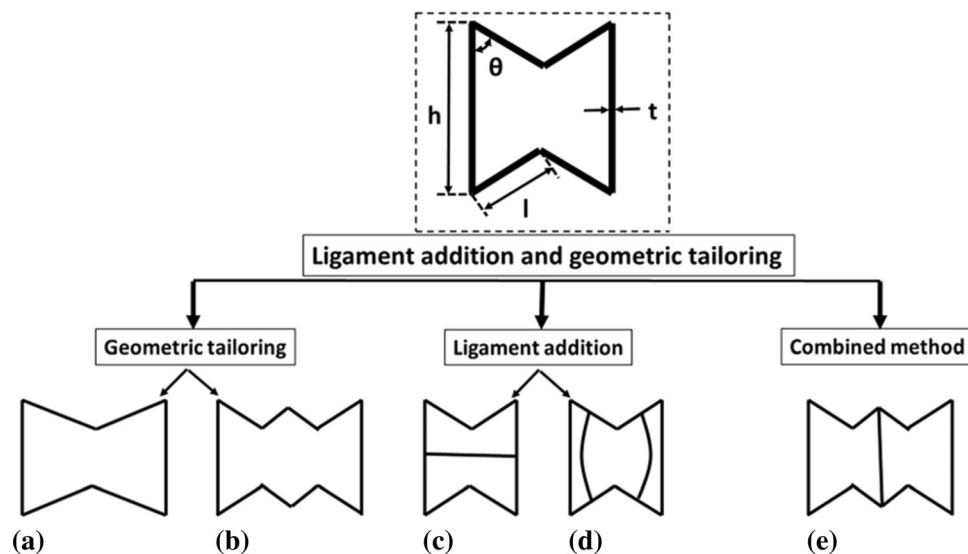


**Fig. 6** Different design methodologies belong to ligament addition and geometric tailoring method: (a) geometric tailoring due to changes in the geometrical parameters, (b) geometric tailoring by splitting the ligaments, (c) ligament addition perpendicular to the straight ligament, (d) ligament addition parallel to the straight ligament and (e) combined method. In all cases, loading direction is parallel to the straight ligament

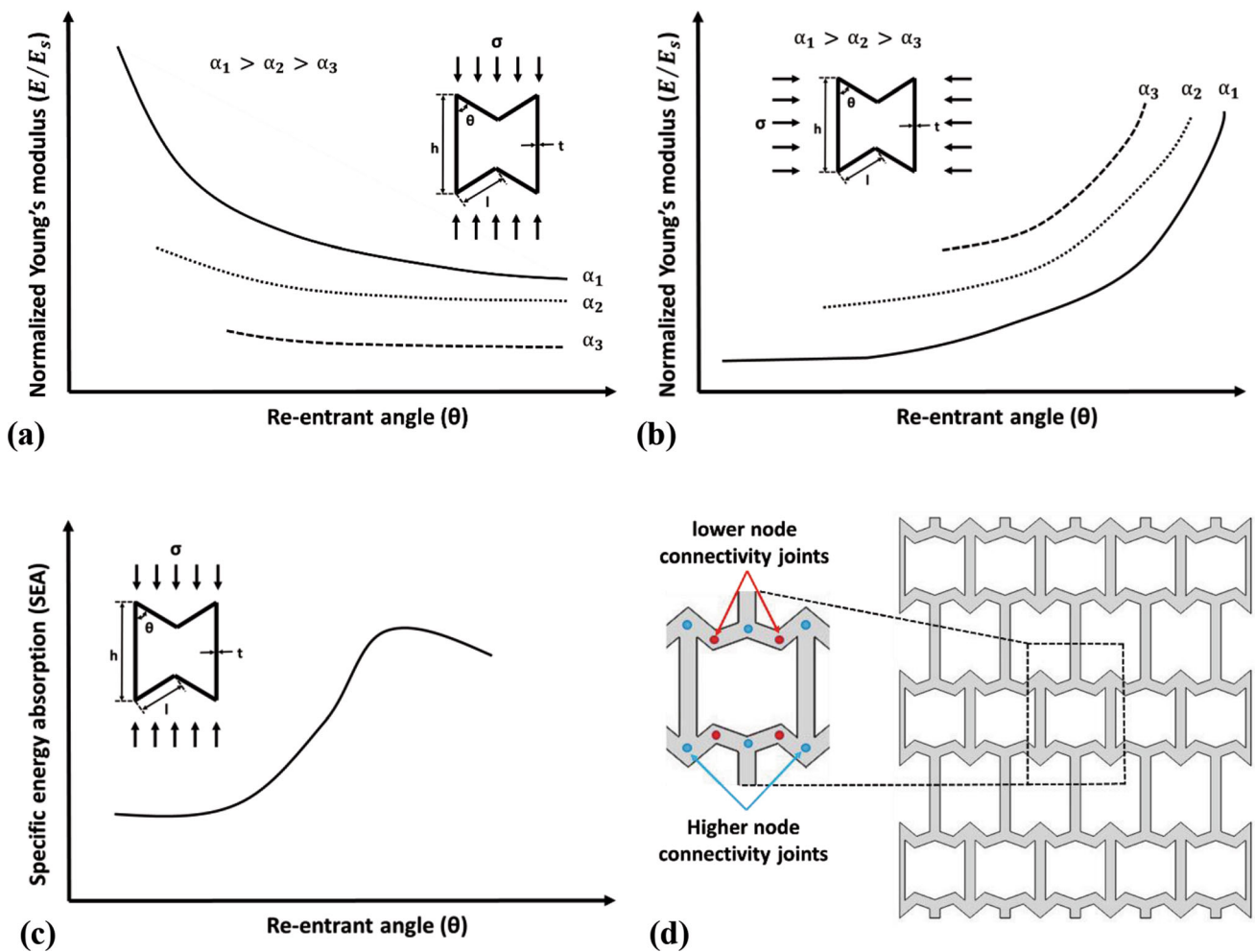


**Fig. 7** Geometric tailoring: (a) effect of re-entrant angle ( $\theta$ ) &  $\alpha$  on the normalized Young's modulus of the re-entrant lattices loaded parallel to the straight ligament, (b) effect of re-entrant angle ( $\theta$ ) &  $\alpha$  on the normalized Young's modulus of the re-entrant lattices loaded perpendicular to the straight ligament, (c) effect of re-entrant angle ( $\theta$ ) on the SEA of the re-entrant lattices loaded parallel to the straight ligament and (d) CAD model with a representative unit cell of the modified re-entrant honeycomb structure showing different types of joints (Ref 29). Panel (d) reprinted from *Composites Part B: Engineering*, Vol 228, Niranjn Kumar Choudhry, Biranchi Panda, S. Kumar, In-plane energy absorption characteristics of a modified re-entrant auxetic structure fabricated via 3D printing, Article 109,437, Copyright 2022, with permission from Elsevier

more dominating as re-entrant angles increase as can be seen in Fig. 7(b).

For both loading conditions, the effect of  $\alpha$  on the normalized Young's modulus is higher at lower re-entrant angles and its effect reduces as re-entrant angles increased. Similar patterns are reported by the researchers who proposed new re-lattice designs by changing the design parameters (Ref 26-28). For all the cases of small re-entrant angles, the normalized Young's modulus is the highest when the loading is parallel to the straight ligament. Thus, the re-entrant angle has a strong influence on the mechanical performance of the re-entrant lattice.

Figure 7(c) shows a relation between the specific energy absorption of re-entrant lattices to the corresponding re-entrant angles for a given value of  $\alpha$  and  $t$ . At a lower value of  $\theta$ , the cell of lattices collapsed very early due to easy contact of the opposite inclined members, leaving behind a porous deformed layer, leading to lower energy absorption with an early onset of densification strain (Ref 29). As the re-entrant angle increased, its specific energy absorption increased and became the

maximum near the re-entrant angle of  $60^\circ$ ; thereafter, a drop in the specific energy absorption capacity of the lattices was observed.

Another way of developing higher energy absorption capacity re-entrant lattices is by introducing lower node connectivity joints (Fig. 7d). These lower node connectivity joints further improve the bending-dominated deformation mode leading to a higher energy absorption capacity of the developed re-entrant lattice. Higher node connectivity joints restrict the movement of inclined ligaments near the joints, while lower node connectivity joints allow easy rotation near the joint due to the lower rotational stiffness of the joint (Ref 3, 29). Local deformation takes place due to the presence of these lower node connectivity joints, which improves the onset of densification strain and hence the energy absorption capacity of resultant re-entrant lattices. Performance of the lattices can be further improved by making them lightweight by removing the masses from inclined ligaments (Ref 30).

In the ligament addition method, straight, zigzag or curved ribs are added parallel or perpendicular to the straight ligaments

(Ref 27, 31, 32) (Fig. 6c and d). The addition of ligaments strongly influences the stiffness of re-entrant structures (Ref 33). It has been found that ligament addition changes the deformation pattern (bending dominated deformation pattern to stretching dominated deformation pattern)(Ref 34) and reduces the auxeticity of the re-entrant structure (Ref 35). The added ligament restricts the lateral movement of the cell and hence reduction in their transverse strain which leads to reduction in auxeticity of the structure. For the same relative density, ligament addition improves the stiffness of the structure but reduces energy absorption capacity due to the formation of the soft post-yield response (Ref 36). Nevertheless, the energy absorption capacity of the structure can be further improved by adding lower wall thickness ligaments that can introduce local buckling effect (Ref 31, 37, 38). In a recent work, ligaments are added only at higher node connectivity joints to simultaneously improve stiffness and energy absorption capability of re-entrant structure. Due to the selective addition of ligaments, Choudhry et al. (Ref 35) observed the enhancement in the stiffness and SEA up to 3.55 and 1.65 times, respectively. Further improvement in stiffness and SEA ( $\sim 4.5$  and  $\sim 3.5$  times, respectively) was achieved by increasing the thickness of the added ligaments marginally.

**2.2.2 Hybrid Re-entrant Structure.** In the hybridization method, new structures are developed by adding two or more different lattice structures. These newly developed structures are called hybrid structures. These hybrid structures are designed in such a way that they can have the advantages of both the parent lattices. The mechanical properties of hybrid structures are found to be higher than that of their parent structures.

Figure 8(a) shows a hybrid re-entrant structure which is designed for higher NPR, and it can sustain larger compressive strain (more opening). A hybrid structure is formed by putting a re-entrant honeycomb within the center of a chiral unit cell (Ref 39). A chiral structure is a structure, which is distinct from its mirror image (Ref 40). Although re-entrant structure is highly auxetic (more NPR) and its auxeticity can be tailored, yet it is not able to sustain larger deformation due to loss in stability and auxeticity after the instability. On the other hand, chiral structures are stable for larger deformations despite having lower auxeticity (lower NPR). The new hybrid design is able to maintain higher auxeticity as well as greater stability for a larger deformation.

Ingrole et al. (Ref 14) designed new structures (Fig. 8b) by combining the honeycomb structure with a re-entrant honeycomb auxetic structure to introduce a local failure (buckling of strut) of the structure during compression. The structure was designed in such a way that it can evenly distribute the applied load throughout the structure. Due to the high thickness (2.5 times that of an inclined strut) of the vertical strut, the structure had enhanced mechanical properties than the parent structures. The pattern of deformation was different than their parent lattices, which concluded that the path of deformation can be changed by changing the topology of the structure and hence desired mechanical property can be achieved. The hybrid structure had improved energy absorption than their parent structures. The improvement in energy absorption was 70% and 30% when compared with honeycomb and re-entrant structures, respectively.

Figure 8(c) shows a narrow-ribs auxetic re-entrant honeycomb hybrid structure. In the narrow-ribs auxetic re-entrant honeycomb hybrid structure, local buckling is induced for

improving the energy absorption capacity of the hybrid lattice by embedding the lower wall thickness rhombus structure (Ref 41). Due to the lower wall thickness of the rhombus structure, the wall of the rhombus lattice buckles more than the original re-entrant wall during compression. This leads to local buckling of struts during the deformation and thus increases the energy absorption (EA) ability of the structure.

**2.2.3 Graded Re-entrant Structure.** Functionally graded materials/structures (FGMs) characterized by a gradual change in a prescribed volume have been frequently used for energy absorption applications (Ref 20, 42, 43). These structures are also known as gradient cell structures. Here, either the cell wall thickness or unit cell size varies from one layer to another layer. Figure 9(a) shows the cell wall angle-graded structure where lattices are designed by varying the cell wall angle to enhance energy absorption capability of the structure (Ref 44). Due to grading in structure, the initial peak stress value is reduced. The deformation wave moves from a weak-to-strong direction which enhances the energy absorption capacity of the graded structure with smaller initial peak stress. The effect of grading is not significant in sequences of crushing deformation, but it affects extensively the local deformation (Ref 45).

**2.2.4 Composite Re-entrant Lattice Structure.** The afore-mentioned design methods are capable of improving the lattice performance to some extent (up to a few-fold) only. Generally, lattices have poor stability and load-carrying capacity due to the presence of cavities. Composite re-entrant lattices can mitigate these problems. This section discusses the mechanical performance of composite re-entrant structures. Figure 9(b) depicts a representative composite lattice structure where the auxetic cell wall is made of stiffer material and internal cavities are filled with soft material (Ref 46). These composite structures have much higher mechanical performance than the structures made up of a single material (Ref 47).

Albertini et al. (Ref 48) developed a composite structure where walls of auxetic lattice were 3D printed using VeroWhite material (opaque white polyjet resin) and cavities were filled with TangoBlack (soft material). The compression test results revealed superior performance of the composite structure in terms of stiffness and energy absorption efficiency. The material filled in the cavity of the auxetic lattice frame is known as matrix; it helps in improving the stiffness and compressive strength due to the biaxial compression of the matrix. Many similar examples were reported in the literature where lattices were fabricated with stiffer material and cavities were filled with soft material (Ref 49-52).

In some cases, auxetic composites are made by filling the lattices with different densities of foamed concrete. The energy absorption capability of foamed concrete influences the energy absorption capability of the composite lattices (Ref 53). It has been reported that the higher density foamed concrete resulted higher energy absorption capability composite lattice. The performance of concrete is also improved by using lattice designs as a reinforcement. Here, the lattices are made from polymer and considered as reinforcement, while concrete is considered a matrix. Due to presence of reinforcement, the load-bearing capacity of concrete composite is increased by many folds (Ref 54). The performance of concrete composites under bending is improved due to the mitigation of concentrated loads and crack deflection.

The conventional lattices are permanently damaged during the compression, but they are not recoverable. New composites

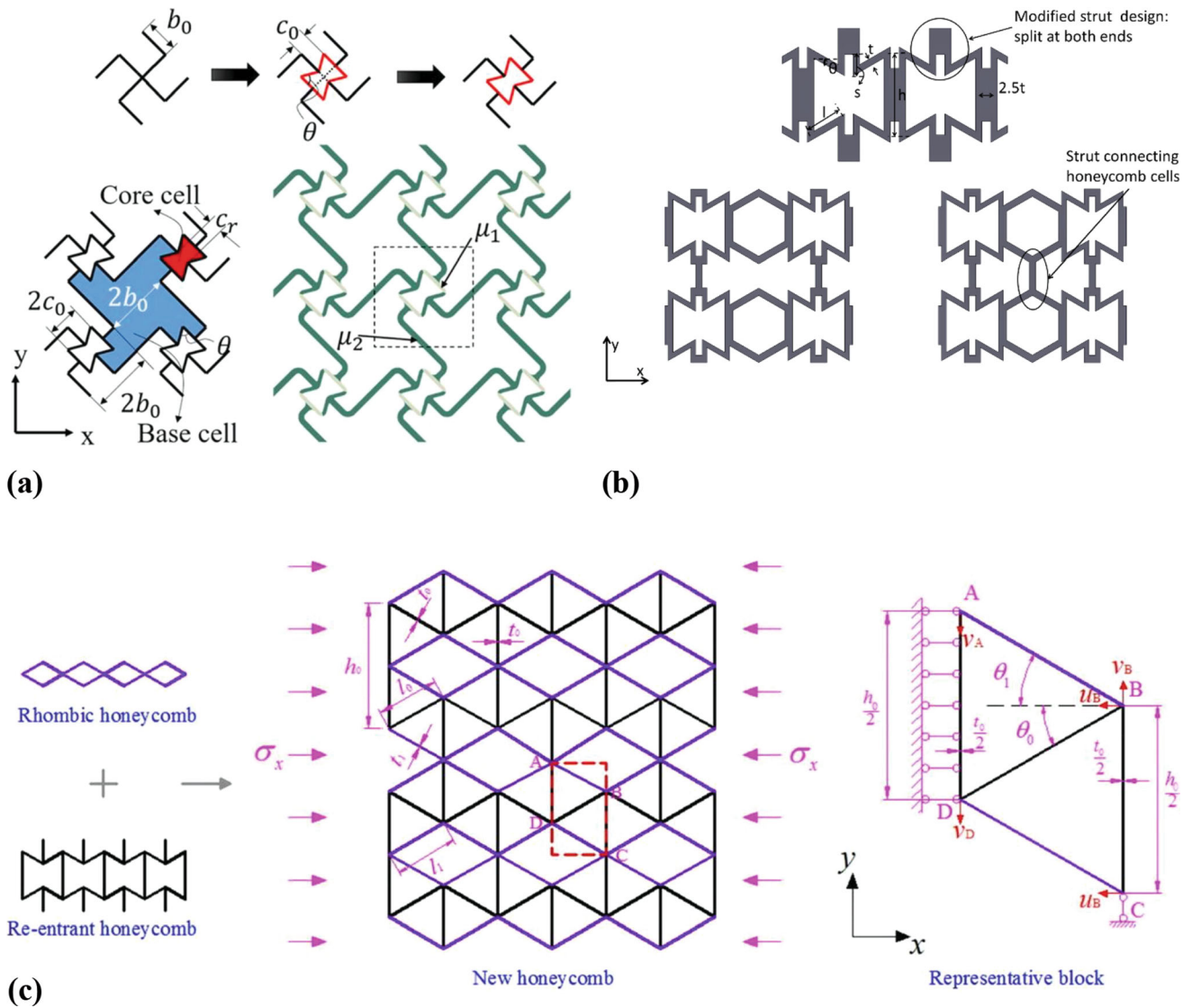


**Fig. 8** Different methods for designing the hybrid re-entrant structure: (a) new chiral cell with re-entrant core cell (Ref 39). (b) Unit cell of hybrid structure as auxetic-struts, auxetic-honeycomb1 (AH-V1) and auxetic-honeycomb 2 (AH-V2) (Ref 14). (c) Narrow-ribs auxetic re-entrant honeycomb structure (Ref 41). Panel (a) reproduced under a Creative Commons Attribution 4.0 International License. Panel (b) reprinted from *Materials & Design*, Vol 117, Aniket Ingrole, Ayou Hao, Richard Liang, Design and modeling of auxetic and hybrid honeycomb structures for in-plane property enhancement, Pages No. 72–83, Copyright 2017, with permission from Elsevier. Panel (c) reprinted from *Composite Structures*, Vol 175, Ming-Hui Fu, Yu Chen, Ling-Ling Hu, Bilinear elastic characteristic of enhanced auxetic honeycombs, Pages No. 101–110, Copyright 2017, with permission from Elsevier

are developed to overcome the permanent damage of auxetic lattices by using the slow recovery foam (Ref 51). The foam acts as a superior buffer material; it has superior energy absorption and high-volume compressibility. Lateral buckling of the structure is minimized. The wall thickness and re-entrant angle also affect the energy absorption of the composite. Energy absorption increases with the wall thickness but reduces with increasing re-entrant angle of the auxetic lattice. These composite structures are used repeatedly without having permanent deformation and hence have many potential engineering applications such as automobile engineering, aerospace, protective engineering and biomedicine.

### 2.3 Sandwich Re-entrant Structures

The sandwich panel structures have been widely used in many industrial applications because of their high mechanical properties. Sandwich panels containing auxetic structure as a core have been designed to prevent the effect of blast at the battlefield. It was observed that auxetic re-entrant honeycomb cored structures have better energy absorption capacity than honeycomb cored structures (Ref 55, 56). The peak reaction force shown by the auxetic cored sandwich panel is lower than the non-auxetic honeycomb core. The deformation pattern of the re-entrant cored sandwich beam has two sections: (I) local compression deformation at the center of the beam and (II) bending-stretching deformation on both sides of the center. The core structure fails due to either local indentation or cell wall



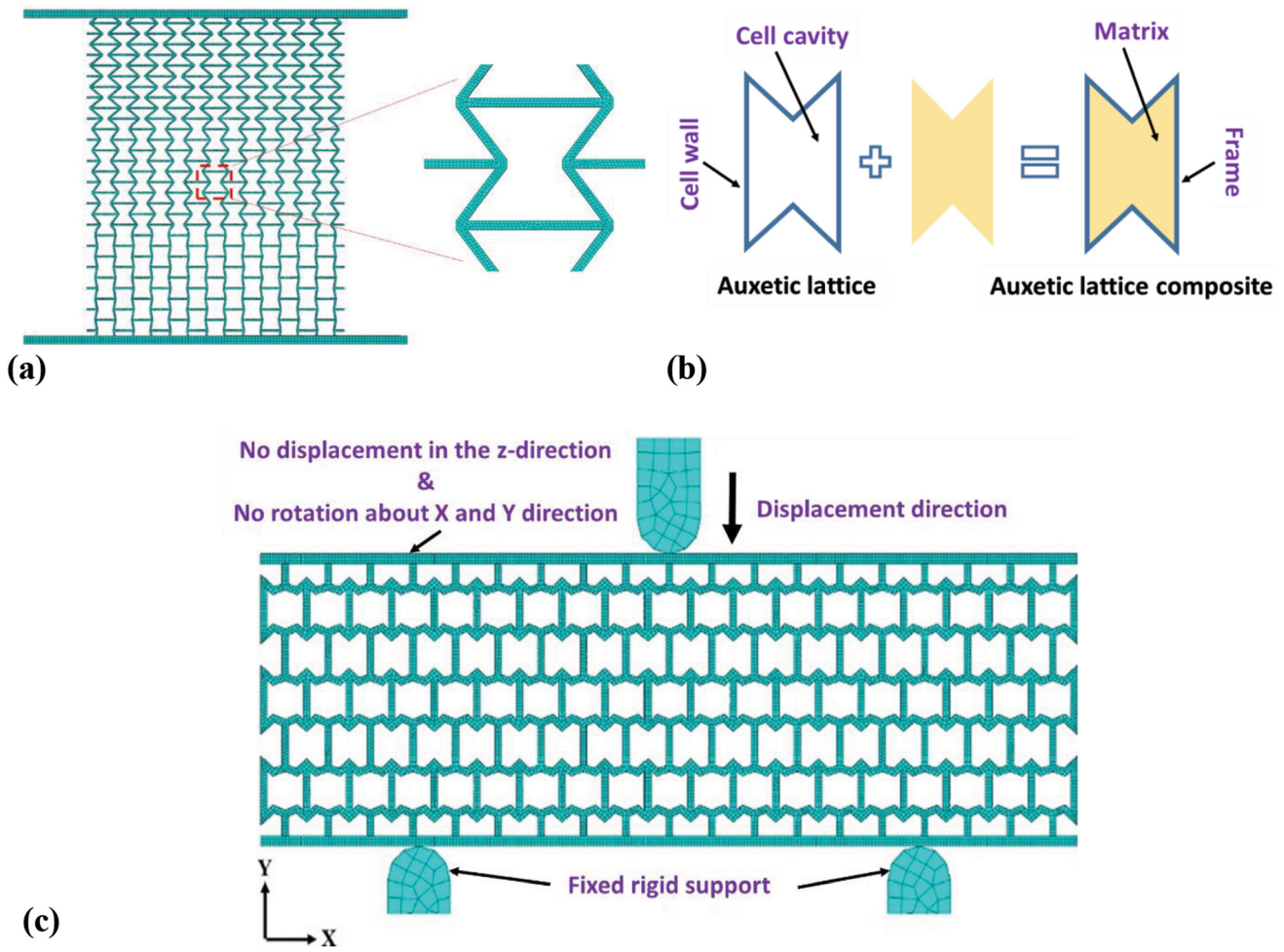


**Fig. 9** FEA model of (a) graded structure (Ref 44). (b) Composite lattice structure and (c) boundary conditions of a sandwich structure having auxetic re-entrant honeycomb structure as a core (Ref 59). Panel (a) reprinted from *Composite Structures*, Vol 247, Xin Wu, Yutai Su, Jing Shi, In-plane impact resistance enhancement with a graded cell wall angle design for auxetic metamaterials, Article 112451, Copyright 2020. Panel (c) reprinted from *Materials Today: Proceedings*, Vol 56, Niranjan Kumar Choudhry, Shailesh Ravindra Bankar, Biranchi Panda, Harpreet Singh, Experimental and numerical analysis of the bending behavior of 3D printed modified auxetic sandwich structures, Pages 1356–1363, Copyright 2022, with permission from Elsevier

fracture or due to shear (Ref 57, 58). Figure 9(c) shows the numerical model developed for analysis of sandwich structure.

Beharic et al. (Ref 60) designed a sandwich structure in which the core of the structure was made from lower stiffness material, while the outer surface was made using rigid material. The purpose of skin is to provide rigidity against bending, while the core provides shear rigidity. By experimental observation, it was clear that impact properties depend on thickness of skin of the sandwich panel, relative density of the core structure and overall thickness of the structure. Tan et al. (Ref 61) designed a sandwich panel with three-layered core structures (re-entrant, re-entrant hierarchical with regular hexagonal honeycomb (RHH) and regular equivalent triangle (RHT)) and found higher energy absorption performance compared to the conventional re-entrants. Ma et al. (Ref 62) developed new sandwich panel where they used a functional-graded auxetic structure as a core material. The frontal facet not only prevents auxetic core as it does not allow blast waves to come in direct contact with the core but also distributes the impulsive load throughout. This leads to high energy absorption and uniform deformation of composite panels.

#### 2.4 4D Printing of Re-entrant Structures

4D printed structures make use of materials such as single-shape memory polymers (SMP), liquid crystal elastomers, composite hydrogel to maintain a temporary shape and return to their original shape with influence from external environment sources such as temperature, pressure, humidity and electromagnetic fields (Ref 63–65). Auxetic structures made by 4D printing process have better tunable mechanical properties such as stiffness, Poisson's ratio, energy absorption and rigidity than those in conventional structures (Ref 66, 67). These smart structures were shaped reconfigurable and reusable with the self-deployable properties. Their stiffness and energy absorption capacity can be adjusted by adjusting the temperature and time (Ref 63, 68).

Shape memory cycle has three major stages—shape programming, fixation and recovery (Ref 68). Shape programming is performed by heating a re-entrant structure to some temperature (say 70 °C for a typical digital SMP) such that SMP material becomes like rubber. At the same elevated temperature, compression is performed, and at the end, a folded honeycomb is built. During fixation, the load is not removed,

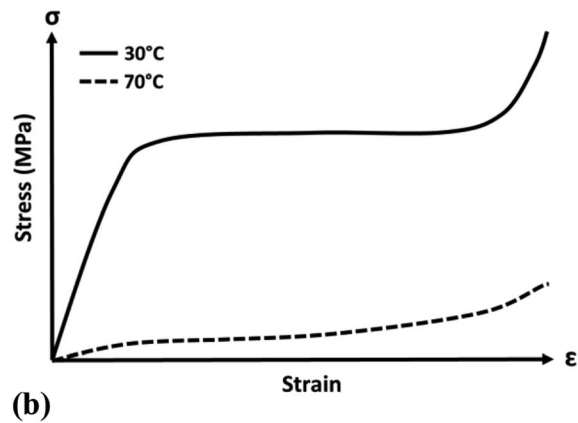
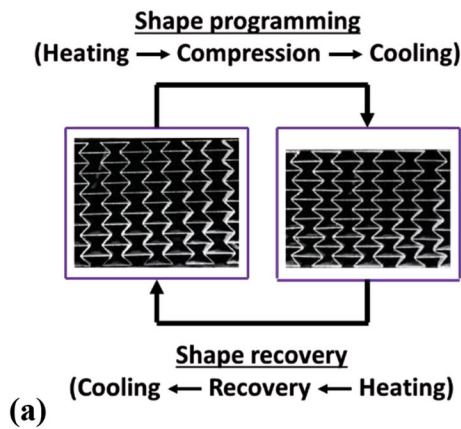


**Fig. 10** SMP and their mechanical performance; (a) shape programming and self-expanding process of SMP re-entrant honeycomb under compressive load and (b) stress–strain response of 4D printed re-entrant lattices at low and high temperatures

but the temperature is lowered to 30 °C so that the material reaches its glassy state. Finally, a deformed honeycomb is retained, which can be further completely recovered to its initial shape by heating it to 70 °C during shape recovery. By adjusting the heating time and temperature during the programming the shape fixation rate can be adjusted; thus, the performance can be monitored. Similarly, the shape recovery rate can also be adjusted by adjusting the heating time and temperature to get the original shape through complete elastic deformation (Ref 63). Figure 10(a) shows the shape programming, fixation and self-expanding process of SMP re-entrant honeycomb under compressive load.

The 4D printed lattices have a similar compressive response as that of 3D printed lattices. They have also three distinct stages at both higher and lower temperatures. In the first stage, deformation is uniform, while in the second stage, structure buckles and distortion starts from the edge of the re-entrant hexagon. At the end, the stresses get elevated because of the densification that occurs in the third stage. Figure 10(b) shows the stress–strain response of 4D printed re-entrant lattices at low and high temperatures. It was observed that the responses of these structures are quite different and hence there is a difference in mechanical properties. Table 1 presents the effect of temperature on Young’s modulus ( $E_t$ ) of the 4D printed re-entrant structure. At higher temperatures, the re-entrant structure showed lower stiffness (1/60 to that at a lower temperature) and higher flexibility. It was also noticed that the properties are adjustable and reversible. By changing the wall thickness, mechanical properties (stiffness/elastic modulus) are significantly changed and the plateau region in stress–strain curve can be further increased by having the repeated compression cycle at a given temperature.

Further, dual-material meta-structures (DMMS) made up of soft (hyper-elastic polymer) and hard (elastoplastic material) materials have better energy absorption (Ref 69, 70). These structures exhibit good capacity to generate nonlinear stiffness for better energy absorption (Ref 71). The dual-material characteristic of these DMMS has the feature of easy dissipation of the energy due to mechanical hysteresis; there is non-coincidence of compressive loading and unloading curves. It has been demonstrated that the plastic deformation and dissipation of energy was completely reversed as these DMMS were heated.

**Table 1** Switching mechanical properties by thermal excitation

Temperature, °C	Young’s modulus, MPa	Change in Young’s modulus, $\frac{E_t}{E_{30^\circ}}$
30	3.4	1.000
40	0.8	0.235
50	0.24	0.070
60	0.096	0.028
70	0.06	0.017

An investigation was made on the auxetic re-entrant structures by applying different programming and recovery cycles at different deformation levels to get varying stiffness and Poisson’s ratio (Ref 66). There was a nonlinear relationship between the modulus of shape memory polymer (SMP) and the level of programming. Due to repetitive cycles of programming and recovery, residual strains got induced in printed structures that led to a reduction in the mechanical properties. Two factors influenced the magnitude of the residual strains, the level of deformation applied during the programming and the number of cycles of programming and recovery.

Large shape transformations were achieved by designing active auxetic metamaterials (AMM) (re-entrant and anti-chiral) (Ref 64). SMP materials were used to 4D print the active auxetic metamaterial. There was around 200% area transformation in AMM due to external stimuli of temperature. The temperature at the recovery step plays a vital role in deciding the rate of shape transformation; greater the temperature, the lesser the time required (10 s at 80 °C).

### 3. Research on Analytical and Numerical Modeling of Re-entrant Structures

With the rapid development of powerful computational techniques, numerical modeling strategies such as finite element method have played an increasingly important role to further understand the performance of deforming lattices. It helps in relating the deformation modes to their mechanical

properties. There are several methods to decode the lattice behavior during compression, which are highlighted in the sequel. Generally, the homogenization technique is used to study mechanical behavior theoretically. In this method, mathematical equations for the coarse-scale phase are derived by considering the geometry of structure and equations derived for fine-scale phases (Ref 72). This technique reduces the design cost and computational time. As the microscopic structural-scale models are converted into an averaged form, the problem can be solved following continuum approach at macroscopic level (Ref 73).

### 3.1 Analytical Modeling

Many mechanics-based models were developed to study the auxetic behavior of re-entrant auxetic structures based on Timoshenko and large deflection beam theories (Ref 74). These models were used for structures having small relative density, i.e., for structures having small ratio of the volume occupied by the solid cell walls to the nominal volume of a cell (Ref 75). The finite element method-based homogenization methods may pose computation difficulties in terms of convergence and computational time (Ref 76, 77). Wang et al. (Ref 24) proposed a strain-based expansion homogenization method for elastic analysis of re-entrant auxetic cellular structure. In-plane elastic modulus and Poisson's ratios were calculated analytically.

Lira et al. (Ref 78) analyzed out-of-plane shear properties of the re-entrant honeycomb structure. A large deflection model was used to derive the expressions for Poisson's ratios for the 2D re-entrant structure. Wan et al. (Ref 79) and Levy et al. (Ref 80) also considered large deflection and expressed Poisson's ratios for the structure in two principal directions. However, many parameters related to the design of structure that affect the Poisson's ratios were ignored. This problem is solved by combining a large deflection beam model with a Timoshenko beam model. Based on homogenization theory and solving partial differential equation, Gonella et al. (Ref 81) estimated the equivalent elastic moduli and Poisson's ratios of structure. The large deformation study of re-entrant structures has also been carried out (Ref 74). For considering the nonlinear behavior in large deformation, a nonlinear modifying factor was used. The model estimated in-plane shear modulus quite accurately. Chan et al. (Ref 82) studied the deformation of conventional and auxetic foams. They also estimated the effect of thinning on the Young's modulus using a classical model of literature. A three-dimensional re-entrant model was developed by Lu et al. (Ref 83) for predicting the Young's modulus and Poisson's ratio of auxetic re-entrant structure.

Analytical models consider some assumptions and developed for individual structures. A generalized model that will fit for all types of structures is not yet reported. It is also difficult to derive analytical expression for complex structures. This prompted researchers to develop numerical models.

### 3.2 Numerical Modeling

FEM was used using ANSYS, LS-DYNA, ABAQUS, etc., and has gained in popularity as one of the most powerful tools to study the deformation behavior of re-entrant honeycomb structure. In order to replicate actual experimental conditions where large deformation was taking place, an "Explicit dynamic" analysis was generally opted with considering all nonlinearity problems (as material nonlinearity, geometric nonlinearity and boundary nonlinearity).

At the early stage, researchers used elastic, elastic-plastic and elastic-perfectly plastic material models to study the crushing response of polymer or metal lattices (Ref 14, 30). These material models only consider the elastic and plastic performance of the base material under tension and are applicable to those materials which have the same yield behavior under tension and compression loading. Polymers that exhibit significantly different yield behavior in tension and compression are modeled by using a pressure-dependent plasticity model such as the linear Drucker-Prager plasticity model (DP) and the volumetric hardening model (VHM) (Ref 29, 84). These material models predict more accurate results and are capable of capturing accurate deformation patterns during the compression of the lattices (Ref 29).

To include and get insight into the crack generation and propagation near the joints and their effect on the failure and delamination of the ligament along with the above-stated models damage models are added (Ref 29, 85) such as Johnson-Cook damage criterion was combined with damage evolution law or linear Drucker-Prager plasticity model (DP) was combined with ductile damage model (Ref 84, 86). As per this model, the failure of the cell follows the following steps. At first, a void nucleates within the cell; thereafter it grows and finally collapses. In the model, it was assumed that the equivalent plastic strain was affected by the following factors: stress triaxiality, pressure stress, von Mises equivalent stress and equivalent plastic strain rate (Ref 87, 88). Many parameters that affect ductile damage are strain rate, plastic strain and temperature. Kramberger et al. (Ref 89) used continuum damage mechanics (CDM) model to study the deformation behavior of auxetic cellular structure.

When a structure is made from a unit cell by arranging it periodically, then the study of mechanical behavior becomes very simple. Instead of taking the whole structure for study we can only consider a unit cell, and periodic boundary conditions are applied. This reduces the simulation cost (Ref 90, 91). This approach is called the infinite medium model approach. On the other hand, in finite medium models, the free surface effects are used to study the mechanical properties where loads are applied in a well-defined way. Loads are applied on the top surface of the structure, and the bottom surface of the structure is fixed. In this case, the top and bottom surfaces are considered rigid plates. Different material models (Ref 18, 92-98) used for numerical modeling of re-entrant structures in recent years are shown in Table 2.

To study the behavior of re-entrant structure different models were proposed by researchers such as 'Beam Element Model' and 'Continuum Element Model.' Beam Element Models consider the element of structure as a 3D element. It considers the effect of bending and transverse shear by using quadratic interpolation functions. The vertex of a cell is assumed to be spherical with high stiffness, and its radius is considered as same as that of the strut radius. Due to the spherical shape, there is an overlap or a gap at the joint of the vertex for the cylindrical strut. Often the stiffness of the structure is over-predicted. However, at the same time, this model is computationally cheap (Ref 99). Continuum Element Models have tetrahedron elements with quadratic interpolation functions and consider all features of the structures which provide a detailed study of the structure. Due to the rapid prototyping process fillets are generated between the struts, these fillets are modeled using the continuum element approach. The length of the element edge is generally lesser



**Table 2 Numerical models used for the analysis of re-entrant structures**

Sr. no.	Structure	Material model	References
1	Cell wall angle-graded auxetic metamaterials	Linear Elastic model	(Ref 44)
2	Re-entrant Circular Honeycomb	Linear-Plasticity material model	(Ref 10)
3	AuxHex lattice structure	Johnson-Cook plasticity material Model	(Ref 100)
4	Auxetic lattice cylindrical structures	Ductile Damage model	(Ref 92)
5	Re-entrant Chiral Auxetic structure	Strain hardening material model	(Ref 18)
6	Re-entrant anti trichiral honeycomb	Elastic perfectly plastic	(Ref 93)
7	Re-entrant representative unit cell as well as a star subordinate cell	Elastic material model	(Ref 94)
8	Double-arrowed auxetic structure	Perfectly elastic plastic	(Ref 95)
9	Hierarchical(slotted) and non-hierarchical structure	Linear plasticity material model	(Ref 96)
10	Re-entrant Star-shaped Honeycomb(RSH)	Elastic perfectly plastic	(Ref 97)
11	Auxetic Re-entrant cells	Elastic-plastic material model	(Ref 98)
12	Re-entrant chiral auxetic	Elastic-plastic material model	(Ref 23)
13	Augmented Re-entrant Honeycomb	Elastic perfectly plastic	(Ref 34)

than 1/6 of the diameter of the strut and mesh refinement occurs at the vertices. The computational cost of the process is very high when compared with Beam Element Models, but at the same time, it provides highly accurate stress and strain fields which helps in studying the mechanical behavior of a structure.

Mechanical properties of re-entrant structures were studied through theoretical and numerical models. These models were developed for in-depth analysis of structural behavior during quasi-static compression. Recently more focus was given to developing numerical models as it gives a clear insight into the deforming structure. Results generated from the numerical model were compared with experiments. The accuracy of results predicted from the model depends on the accuracy of the model.

#### 4. Fused Deposition Modeling 3D Printing

Lattice designs are very complex for manufacturing and cannot be precisely manufactured using conventional manufacturing processes. The 3D printing methods are best suited for the fabrication of such complex geometry with a size of micro-to macroscale. The process involves in the deposition of material in a layer-by-layer manner directly from CAD model (Ref 101, 102). With the advancement of technology, 3D printing processes (Ref 103, 104) including (Table 3) poly jet (Ref 105, 106), stereolithography (SLA) (Ref 107-109), fused deposition modeling (FDM) (Ref 110-118), SLS (Ref 119), SLM (Ref 120-122) and direct wire 3D printing are becoming sustainable in terms of material utilization and productivity. From Table 3 it is clear that the FDM method is widely used by many researchers among all other 3D printing processes to fabricate different re-entrant structures.

The FDM method is commonly used to fabricate intricate structures with a thermoplastic material like polylactic acid (PLA) and acrylonitrile butadiene styrene (ABS). A heated semi-liquid filament is extruded out from the nozzle onto the bed of the printer or on the top of the previously printed layer (Ref 123). The minimum size limit of this process depends on the nozzle diameter used for the printer and can be up to a few hundred micrometers (Ref 124). The quality of the printed structure largely depends on the printing parameters for example nozzle diameter, layer thickness, extrusion tempera-

ture, printing speed, infill density and infill patterns (Ref 125, 126).

Due to layer-wise printing, a printed part can have many layers. These layers are responsible for deviation in diameter at different locations of a printed vertical and inclined ligament, and a staircase effect was seen while printing of inclined ligament as shown in Fig. 11(a), which leads to a lower mechanical property when compared to its FEA model (Ref 127). To minimize this difference in numerical and experimental results Ravari et al. (Ref 128) generated a solid non-uniform diameter strut similar to FDM printed part by dividing the length of the strut into N equal parts. Further defects like voids and gaps (improper filling at narrow sections) are common in FDM printing and can be minimized by selecting optimum printing parameters.

FDM was also used to print a re-entrant structure with multi-materials by adding multiple nozzles in it (Ref 130). Johnston et al. (Ref 129) used PLA, PLA-Nylon and PLA-Thermoplastic Polyurethane (TPU) to print different re-entrant structures. It was found that multi-material printed structures failed due to weak layer adhesion (Fig. 11b) rather than material failure (Ref 131). The continuous start and stop of the material extrusion via nozzle caused fine strings (Fig. 11c) within the structure. This interlayer adhesion can be improved by controlling the overlap percentage which will increase the bonding surface area (Ref 131). Despite widespread usage of the FDM printing process, some challenges such as part inaccuracy, higher printing time, less variety of printing material and low productivity need further attention (Ref 129).

#### 5. Industrial Applications of 3D Printed Auxetic Structures

There are many examples of industrial applications of auxetic structures due to their excellent properties such as energy absorption, lightweight, negative Poisson's ratio, relative density, high stiffness, high strength, load bearing, elastic modulus, shape programming, self-deployable, high impact strength, energy dissipation, sound absorption, piezoresistive sensitivity, vibration isolation and energy storage. In this section, only re-entrant structures fabricated by FDM process are discussed for applications in automobile, aerospace, bio-



**Table 3 Summary of additive manufacturing method**

Manufacturing method classification	Manufacturing process	Re-entrant structure type	Material	References
Additive manufacturing method	Poly jet	2D re-entrant graded structures	Stratasys FLX9895-DM and Stratasys VeroWhiteTM	(Ref 44)
		2D re-entrant	VeroWhite and TangoPlus	(Ref 105)
	SLA	2D re-entrant	VeroWhitePlus and TangoBlackPlus	(Ref 39)
			Photosensitive resin	(Ref 106)
	FDM	Cylindrical re-entrant cell 2D star-square structure 2D re-entrant honeycomb 2D re-entrant and arrowed Cylindrical re-entrant cell	High-temperature resistance photosensitive resin HTL®	(Ref 107)
			White elastic brittle photopolymer (EBP)	(Ref 108)
			Photosensitive resin made of BMF material	(Ref 109)
			Tape of polylactic acid (PLA) reinforced with flax fiber filaments (PFF)	(Ref 110)
			Nylon	(Ref 111)
			White thermoplastic elastomer (TPE)	(Ref 108)
	SLM	Graded re-entrant structure Auxetic meta-biomaterials 2D auxetic, re-entrant honeycomb	Poly(lactic acid (PLA) polymer	(Ref 112, 113)
			Thermoplastic polyurethane filament	(Ref 114)
			ABS	(Ref 115-118)
			Aluminum powder AISi10Mg	(Ref 120)
Ti-6Al-4 V powder			(Ref 121)	
Spherical Inconel 718 powder			(Ref 122)	

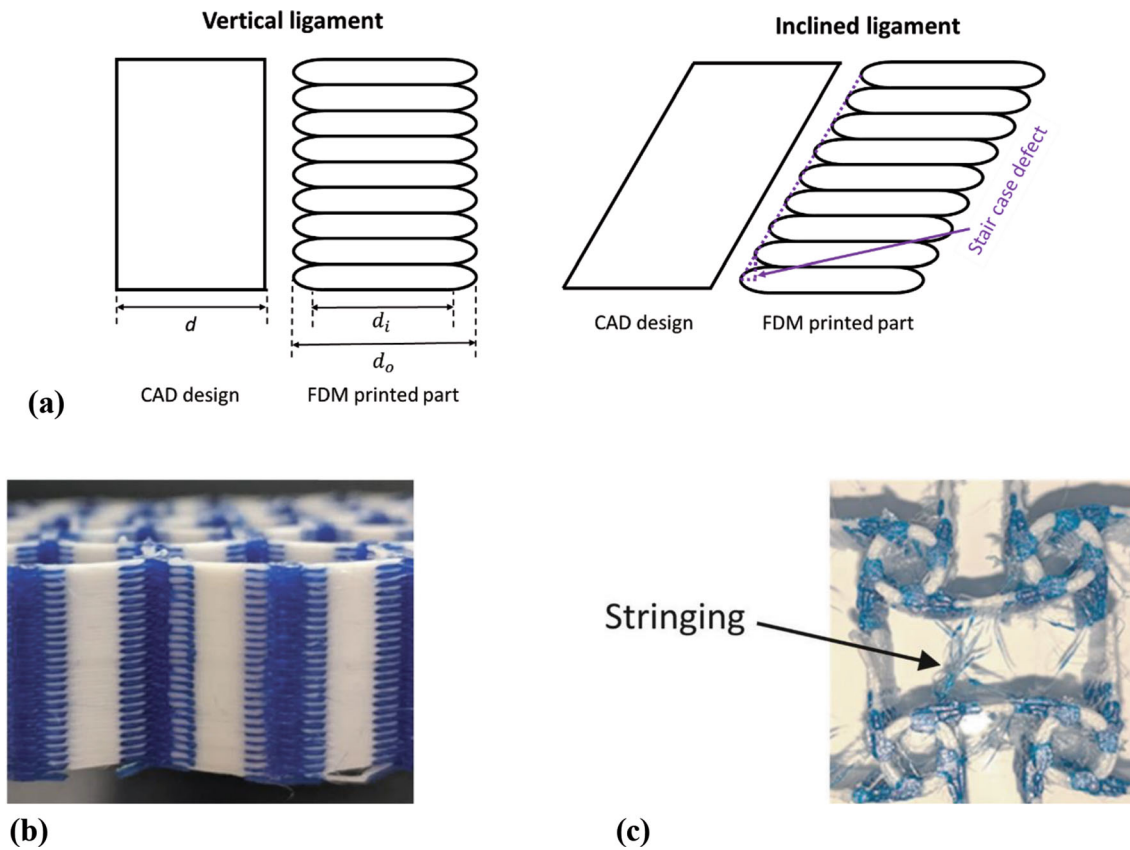


**Fig. 11** Parts printed from FDM printing; (a) defect presented in vertical and inclined ligaments, (b) dual-material splicing (Ref 129), (c) string on print (Ref 129). Panels (b) and (c) reprinted from *Additive Manufacturing*, Vol 38, Ross Johnston, Zafer Kazancı, Analysis of additively manufactured (3D printed) dual-material auxetic structures under compression, Article 101783, Copyright 2021, with permission from Elsevier

medical, defense, marine, offshore, constructions, transportation, sports, textiles, electrical and robotics.

### 5.1 Automobile Industry

There is an increasing interest in designing lightweight automobile parts to enhance the passive safety of automobiles. In vehicle, a crash box structure is an integral component for ensuring the safety of a car which serves as an energy-absorbing member, together with the bumper beam in case of frontal collision during car accidents (Fig. 12a). In this regard, different lattices have been designed and tested in impact and blast loading condition (Ref 132-134). The core of the sandwich was made from auxetic lattices that helped in energy absorption (Ref 135).

Cellular structures (hexagonal and re-entrant) were further used in noise reduction application. The noise produced by automobiles can cause discomfort during hearing, and to mitigate this problem, sound-absorbing devices were designed by using cellular lattices (Ref 136). The cellular structures were fabricated by using polylactic acid reinforced with chicken keratin materials and were capable of reducing noise as they reduced the free space and hence the airflow through themselves.

### 5.2 Bio-medical

Recently, auxetic re-entrant structures were proposed for designing mechanical adjustable stents, smart bandages, bone

screws, bone plates, hip joints (Ref 137-139). Bone screws are the most commonly used orthopedic implants. Auxetic structured screw possesses the advantage, as it expands in a transverse direction when stretched (Ref 140). This helps in improving the fixation contact area of a screw to the bone (Ref 141). Similarly, auxetic structures are proposed for enhancing the radial expansion ability while reducing the axial expansion ability of the stents, used in health problems such as blockage of blood vessels, respiratory tracts because of diseases like cancers, clotting of blood (Ref 142).

Leung et al. (Ref 143) proposed a new heel pad design based on auxetic (Fig. 12b) structure to reduce the pressure on the heel for diabetes mellitus. The heel pad was designed with a circular auxetic RH pattern and fabricated through 3D printing technology. When a compressive load is applied (during walking), the heel pad allows more contact area between the heel pad and foot due to lateral shrinking, and hence, the peak contact force is reduced. It is reported that 10% reduction in peak contact force can be obtained using the proposed design than that of other foam materials.

### 5.3 Aerospace

For impact energy absorption, lightweight sandwich panels are commonly used in aerospace industry. In sandwich panels, the core structure plays a very important role and inspired by advantage of NPR structure, auxetic designs are proposed for energy absorption applications (Ref 61). For curved-shaped parts, sandwich panel composites can be easily formed into

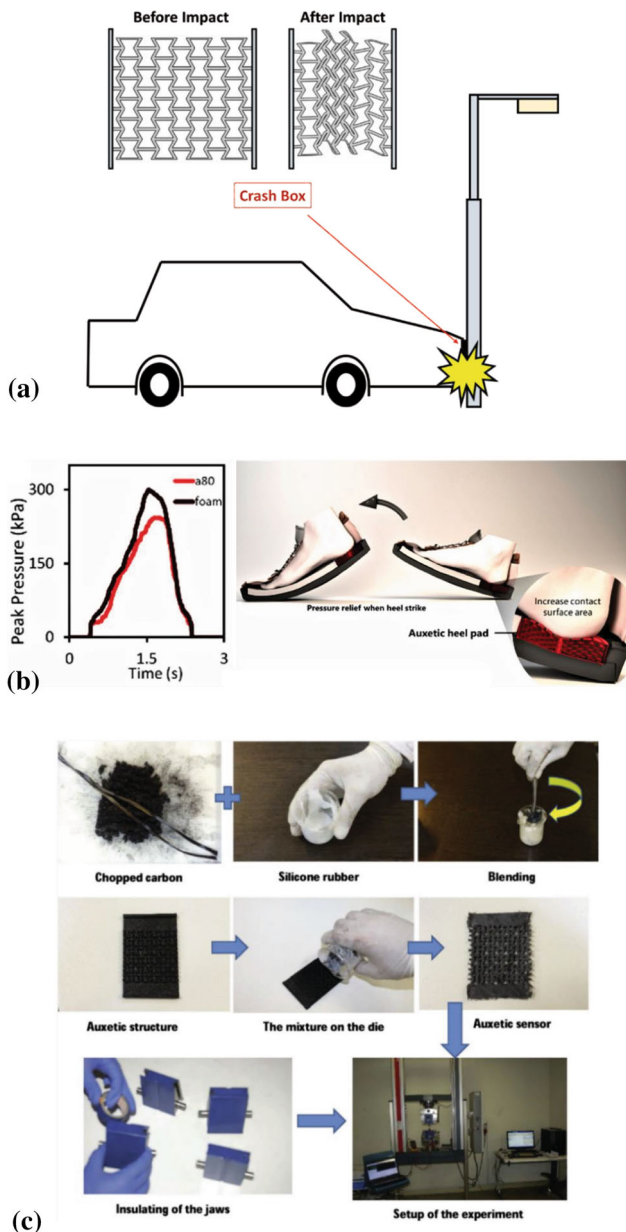


**Fig. 12** Industrial applications of 3D printed auxetic structures; (a) frontal collision during car accidents, (b) peak plantar heel pressure: heel pads with auxetic structure versus PU foam heel pad, and illustration of plantar heel contact during wear trial (Ref 143) (c). Schematic view of the fabrication of highly sensitive piezoresistive sensors in low strain values (Ref 144). Panel (b) reprinted from *Computers in Biology and Medicine*, Vol 146, Matthew Sin-hang Leung, Kit-lun Yick, Yue Sun, Lung Chow, Sun-pui Ng, 3D printed auxetic heel pads for patients with diabetic mellitus, Article 105582, Copyright 2022, with permission from Elsevier. Panel (c) reprinted from *Sensors and Actuators A: Physical*, Vol 305, Bahman Taherkhani, Mohammad Bagher Azizkhani, Javad Kadkhodapour, Ali Pourkamali Anaraki, Shima Rastgordani, Highly sensitive, piezoresistive, silicone/carbon fiber-based auxetic sensor for low strain values, Article 111939, Copyright 2020, with permission from Elsevier

domed shapes and their design can be tailored for high in- and out-plane modulus properties (Ref 137). Auxetic material also finds applications for reducing noise inside the aircraft (Ref 145).

## 5.4 Electrical and Electronics

With the growing interest in electric vehicles, there is an urgent need to ensure the safety of the battery using a battery protector that must have high energy absorption capability and high strength. The re-entrant structured sandwich panels were best suitable for battery storage systems (Ref 146).

Flexible stretchable strain sensors (as shown in Fig. 12c) have many applications in robotics, healthcare monitoring, electric skin and wearable devices due to their larger strain monitoring capacity (Ref 144). The sensor converts mechanical movement into electrical signals. It has two parts first flexible substrates and second sensing materials. To increase the stretchability and improvement in sensitivity of the flexible stretchable strain sensor, flexible substrates were designed by using the re-entrant auxetic structure (Ref 144, 147). This improves stretchability by 98% and sensitivity by 24 times more than the conventional sensors. These sensors have high sensitivity at even low strain and can be used for lower strain conditions like vocal cord dysfunctions, wrist pulses and vibrations of earth, etc. Piezoelectric sensors are also using 2D re-entrant auxetic structures. Sensor frames are made from re-entrant lattices and filled with ceramic (PZT) or soft filler material (silicon rubber) (Ref 148, 149). These sensors have an orthotropic strain response and NPR.

## 5.5 Other Applications

In addition to automobile, aerospace, medical and electronics sectors, FDM printed auxetic structures are found to have very few applications in textile, acoustic [Ref. 150–152] and civil engineering structures. New fabrics were developed based on auxeticity effect by using flat knitting technology with auxetic re-entrant structures (Ref 153). Such new fabric had more flexibility and comfort and was used as sports wearables. Auxetic structures are also used in oil separation where liquid-repellent surfaces and membranes are made from auxetic lattices (Ref 154). With the use of 4D printing, many components were made, which were capable of doing shape recovery (shape programming), self-deployment process, switching stiffness, etc. (Ref 63). These structures are mainly used in mechanical damping devices for automobile applications, morphing wings for aerospace and defense applications, soft robots for robotic-related operations.

## 6. What Remains to be Done?

There are large number of FDM printed two-dimensional re-entrant structures that can provide a range of different auxetic behaviors. Several of these structures have been investigated thoroughly in the literature, providing indications on mechanical properties such as energy absorption. However, no clear comparisons have been made that provide a more direct indication on which structures would be more suitable for a specific application. Although some authors have proposed application specific new re-entrant designs, there are still a number of challenges that need to be overcome for the final utilization of 3D printed lattice structures. This includes defects in parts such as pores, lack of adhesion, poor surface finish and anisotropic properties. The surface roughness characteristics of FDM 3D printed are not acceptable in many applications, and thus, it requires improvement. Anisotropic structure–property

relationship is also non-negligible in FDM printing, which is caused due to layer-wise manufacturing and interfacial issues. Since new studies are focusing on the printing of multi-material auxetic structures, it is worth considering the interfacial adhesion issues between the multi-materials. Special attention needs to be paid for optimization of the process parameters and part post-processing by considering more factors such as environmental factors of the real-life applications.

It has been shown that numerical modeling method is gaining growing attention in recent years. The detailed deformation of re-entrant structures could be better scrutinized through the finite element models. Nevertheless, there is lack of new studies integrating the finite element method with machine learning and artificial intelligence techniques. These data-driven techniques have the capability to capture the stochastic nature of the 3D printing process, which is highly important for producing robust and repeatable part properties. On a similar note, new finite element models should be developed to count the anisotropic nature of the 3D printed part for the accurate prediction of part properties. It is expected that machine learning-guided finite element studies can result in the discovery of new unit cells with improved energy absorption performance. New research directions are also needed for designing bio-inspired energy absorption structures as they offer distinctive deformation behavior than manmade structures. Most researches on re-entrant structures focus on usage of single material, and composite structures with auxetic effect are still in infancy. Ultimately, development of new materials for 3D and 4D printing will provide substantial motivation for developing new light weight structures for multi-functional applications.

## 7. Conclusions

The paper gives an overview of the energy absorption performance of different auxetic re-entrant structures made by FDM 3D/4D printing technique. The numerical models that can capture the unique deformation of the structures under quasi-static loading conditions are discussed. Excellent progress has been made in 3D printing of re-entrant structures by using the ABS polymer due to the low cost and available of wide range of ABS composites. Through simulation and experimental methods, the deformation mechanisms, including the effects of geometrical parameters, have been gradually clarified, promoting a deeper understanding of the material architecture under different loading conditions. Their application has been expanded to various fields such as sandwich plates, smart bandages, sensors, implants and bone screws. Finally, the challenges and opportunities on the FDM printed auxetic structures are discussed to inspire future research work. It is anticipated that this review will help to get insights into the existing auxetic re-entrant configurations, their energy absorption properties for broad engineering applications.

## References

1. X. Ren, R. Das, P. Tran et al., Auxetic metamaterials and structures: a review, *Smart Mater. Struct.*, 2018, **27**, p 23001

2. S. Linforth, T. Ngo, P. Tran et al., Investigation of the auxetic oval structure for energy absorption through quasi-static and dynamic experiments, *Int. J. Impact Eng.*, 2021, **147**, p 103741. <https://doi.org/10.1016/j.ijimpeng.2020.103741>
3. L.J. Gibson and M.F. Ashby, *Cellular Solids: Structure and Properties*, Cambridge University Press, Cambridge, 1999
4. M. Askari, D.A. Hutchins, P.J. Thomas et al., Additive manufacturing of metamaterials: a review, *Addit. Manuf.*, 2020, **36**, p 101562. <https://doi.org/10.1016/j.addma.2020.101562>
5. K.E. Evans, M.A. Nkansah, I.J. Hutchinson, and S.C. Rogers, Molecular network design, *Nature*, 1991, **353**, p 124
6. F. Robert, An isotropic three-dimensional structure with Poisson's ratio = -1, *J. Elast.*, 1985, **15**, p 427–430
7. Q.M. Li, I. Magkiriadis, and J.J. Harrigan, Compressive strain at the onset of densification of cellular solids, *J. Cell Plast.*, 2006, **42**, p 371–392
8. X. Zhang, H. Hao, R. Tian et al., Quasi-static compression and dynamic crushing behaviors of novel hybrid re-entrant auxetic metamaterials with enhanced energy-absorption, *Compos. Struct.*, 2022, **288**, p 115399. <https://doi.org/10.1016/j.compstruct.2022.115399>
9. W. Zhang, S. Zhao, F. Scarpa et al., In-plane mechanical behavior of novel auxetic hybrid metamaterials, *Thin-Walled Struct.*, 2021 <https://doi.org/10.1016/j.tws.2020.107191>
10. C. Qi, F. Jiang, A. Remennikov et al., Quasi-static crushing behavior of novel re-entrant circular auxetic honeycombs, *Compos. Part B Eng.*, 2020, **197**, p 108117. <https://doi.org/10.1016/j.compositesb.2020.108117>
11. J. Zhang, G. Lu, and Z. You, Large deformation and energy absorption of additively manufactured auxetic materials and structures: a review, *Compos. Part B Eng.*, 2020, **201**, p 108340. <https://doi.org/10.1016/j.compositesb.2020.108340>
12. A. Alomarah, D. Ruan, and S. Masood, Tensile properties of an auxetic structure with re-entrant and chiral features—a finite element study, *Int. J. Adv. Manuf. Technol.*, 2018, **99**, p 2425–2440. <https://doi.org/10.1007/s00170-018-2637-y>
13. D. Li, J. Yin, L. Dong, and R.S. Lakes, Strong re-entrant cellular structures with negative Poisson's ratio, *J. Mater. Sci.*, 2018, **53**, p 3493–3499. <https://doi.org/10.1007/s10853-017-1809-8>
14. A. Ingrole, A. Hao, and R. Liang, Design and modeling of auxetic and hybrid honeycomb structures for in-plane property enhancement, *Mater. Des.*, 2017, **117**, p 72–83. <https://doi.org/10.1016/j.matdes.2016.12.067>
15. L.J. Gibson and F.M. Ashby [Lorna J. Gibson, Michael F. Ashby] *Cellular Solid*(z-lib.org).pdf. Cambridge Solid State Sci. Ser. (1997)
16. C. Quan, B. Han, Z. Hou et al., 3D printed continuous fiber reinforced composite auxetic honeycomb structures, *Compos. Part B Eng.*, 2020, **18**, p 7. <https://doi.org/10.1016/j.compositesb.2020.107858>
17. L. Bai, C. Gong, X. Chen et al., Mechanical properties and energy absorption capabilities of functionally graded lattice structures: experiments and simulations, *Int. J. Mech. Sci.*, 2020 <https://doi.org/10.1016/j.ijmecsci.2020.105735>
18. A. Alomarah, S.H. Masood, I. Sbarski et al., Compressive properties of 3D printed auxetic structures: experimental and numerical studies, *Virtual Phys. Prototyp.*, 2020, **15**, p 1–21. <https://doi.org/10.1080/17452759.2019.1644184>
19. Z. Dong, Y. Li, T. Zhao et al., Experimental and numerical studies on the compressive mechanical properties of the metallic auxetic reentrant honeycomb, *Mater. Des.*, 2019, **182**, p 108036
20. J.X. Qiao and C.Q. Chen, Impact resistance of uniform and functionally graded auxetic double arrowhead honeycombs, *Int. J. Impact Eng.*, 2015, **83**, p 47–58
21. W.M. Zhang, Z.Y. Li, J.S. Yang et al., A lightweight rotationally arranged auxetic structure with excellent energy absorption performance, *Mech. Mater.*, 2022 <https://doi.org/10.1016/j.mechmat.2022.104244>
22. M. Najafi, H. Ahmadi, and G. Liaghat, Experimental investigation on energy absorption of auxetic structures, *Mater. Today Proc.*, 2019, **34**, p 350–355. <https://doi.org/10.1016/j.matpr.2020.06.075>
23. A. Alomarah, S.H. Masood, and D. Ruan, Out-of-plane and in-plane compression of additively manufactured auxetic structures, *Aerosp. Sci. Technol.*, 2020, **106**, p 106107. <https://doi.org/10.1016/j.ast.2020.106107>



24. T. Wang, L. Wang, Z. Ma, and G.M. Hulbert, Elastic analysis of auxetic cellular structure consisting of re-entrant hexagonal cells using a strain-based expansion homogenization method, *Mater. Des.*, 2018, **160**, p 284–293
25. T. Baran and M. Öztürk, In-plane elasticity of a strengthened re-entrant honeycomb cell, *Eur. J. Mech. A/Solids*, 2020 <https://doi.org/10.1016/j.euromechsol.2020.104037>
26. S. Vyavahare and S. Kumar, Numerical and experimental investigation of FDM fabricated re-entrant auxetic structures of ABS and PLA materials under compressive loading, *Rapid Prototyp. J.*, 2021, **27**, p 223–244. <https://doi.org/10.1108/RPJ-10-2019-0271>
27. K. Zied, M. Osman, and T. Elmahdy, Enhancement of the in-plane stiffness of the hexagonal re-entrant auxetic honeycomb cores, *Phys. Status Solidi Basic Res.*, 2015, **252**, p 2685–2692. <https://doi.org/10.1002/pssb.201552164>
28. L. Yang, O. Harrysson, H. West, and D. Cormier, Modeling of uniaxial compression in a 3D periodic re-entrant lattice structure, *J. Mater. Sci.*, 2013, **48**, p 1413–1422. <https://doi.org/10.1007/s10853-012-6892-2>
29. N.K. Choudhry, B. Panda, and S. Kumar, In-plane energy absorption characteristics of a modified re-entrant auxetic structure fabricated via 3D printing, *Compos. Part B Eng.*, 2022, **228**, p 109437
30. N.K. Choudhry and B. Panda B, in *Mechanical properties of 3D printed modified auxetic structure: experimental and finite element study*. Low cost manufacturing technologies: proceedings of NERC 2022. (Springer, 2023), pp. 189–200
31. Z.X. Lu, X. Li, Z.Y. Yang, and F. Xie, Novel structure with negative Poisson's ratio and enhanced Young's modulus, *Compos. Struct.*, 2016, **138**, p 243–252. <https://doi.org/10.1016/j.compstruct.2015.11.036>
32. Y. Zhu, Y. Luo, D. Gao et al., In-plane elastic properties of a novel re-entrant auxetic honeycomb with zigzag inclined ligaments, *Eng. Struct.*, 2022, **268**, p 114788. <https://doi.org/10.1016/j.engstruct.2022.114788>
33. Z. Chen, X. Wu, Y.M. Xie et al., Re-entrant auxetic lattices with enhanced stiffness: a numerical study, *Int. J. Mech. Sci.*, 2020 <https://doi.org/10.1016/j.ijmecsci.2020.105619>
34. X. Li, Q. Wang, Z. Yang, and Z. Lu, Novel auxetic structures with enhanced mechanical properties, *Extrem. Mech. Lett.*, 2019, **27**, p 59–65
35. N.K. Choudhry, B. Panda, and S. Kumar, Enhanced energy absorption performance of 3D printed 2D auxetic lattices, *Thin-Walled Struct.*, 2023, **186**, p 110650
36. V.S. Deshpande and N.A. Fleck, Isotropic constitutive models for metallic foams, *J. Mech. Phys. Solids*, 2000, **48**, p 1253–1283
37. M.H. Fu, Y. Chen, and L.L. Hu, A novel auxetic honeycomb with enhanced in-plane stiffness and buckling strength, *Compos. Struct.*, 2017, **160**, p 574–585. <https://doi.org/10.1016/j.compstruct.2016.10.090>
38. L. Boldrin, S. Hummel, F. Scarpa et al., Dynamic behaviour of auxetic gradient composite hexagonal honeycombs, *Compos. Struct.*, 2016, **149**, p 114–124
39. Y. Jiang and Y. Li, 3D printed auxetic mechanical metamaterial with chiral cells and re-entrant cores, *Sci. Rep.*, 2018, **8**, p 1–11
40. N. Novak, L. Krstulović-Opara, Z. Ren, and M. Vesenjak, Compression and shear behaviour of graded chiral auxetic structures, *Mech. Mater.*, 2020, **148**, p 103524
41. M.-H. Fu, Y. Chen, and L.-L. Hu, Bilinear elastic characteristic of enhanced auxetic honeycombs, *Compos. Struct.*, 2017, **175**, p 101–110
42. C.J. Shen, G. Lu, and T.X. Yu, Dynamic behavior of graded honeycombs—a finite element study, *Compos. Struct.*, 2013, **98**, p 282–293
43. J. Plocher and A. Panesar, Effect of density and unit cell size grading on the stiffness and energy absorption of short fibre-reinforced functionally graded lattice structures, *Addit. Manuf.*, 2020 <https://doi.org/10.1016/j.addma.2020.101171>
44. X. Wu, Y. Su, and J. Shi, In-plane impact resistance enhancement with a graded cell-wall angle design for auxetic metamaterials, *Compos. Struct.*, 2020, **247**, p 112451
45. B. Yu, B. Han, P.-B. Su et al., Graded square honeycomb as sandwich core for enhanced mechanical performance, *Mater. Des.*, 2016, **89**, p 642–652
46. R. Yu, W. Luo, H. Yuan et al., Experimental and numerical research on foam filled re-entrant cellular structure with negative Poisson's ratio, *Thin-Walled Struct.*, 2020, **153**, p 106679. <https://doi.org/10.1016/j.tws.2020.106679>
47. X. Ren, Y. Zhang, C.Z. Han et al., Mechanical properties of foam-filled auxetic circular tubes: experimental and numerical study, *Thin-Walled Struct.*, 2022, **170**, p 108584
48. F. Albertini, J. Dirrenberger, C. Sollogoub et al., Experimental and computational analysis of the mechanical properties of composite auxetic lattice structures, *Addit. Manuf.*, 2021, **47**, p 102351
49. Y. Xue, W. Wang, and F. Han, Enhanced compressive mechanical properties of aluminum based auxetic lattice structures filled with polymers, *Compos. Part B Eng.*, 2019, **171**, p 183–191. <https://doi.org/10.1016/j.compositesb.2019.05.002>
50. N. Novak, L. Krstulović-Opara, Z. Ren, and M. Vesenjak, Mechanical properties of hybrid metamaterial with auxetic chiral cellular structure and silicon filler, *Compos. Struct.*, 2020 <https://doi.org/10.1016/j.compstruct.2019.111718>
51. H.C. Luo, X. Ren, Y. Zhang et al., Mechanical properties of foam-filled hexagonal and re-entrant honeycombs under uniaxial compression, *Compos. Struct.*, 2022, **280**, p 114922. <https://doi.org/10.1016/j.compstruct.2021.114922>
52. H.H. Xu, H.C. Luo, X.G. Zhang et al., Mechanical properties of aluminum foam filled re-entrant honeycomb with uniform and gradient designs, *Int. J. Mech. Sci.*, 2023, **244**, p 108075. <https://doi.org/10.1016/j.ijmecsci.2022.108075>
53. S. Wang, Y. Wang, F. Yu et al., Evaluation of in-plane crushing performance of printed randomly polymeric honeycombs filled with foamed concrete, *Constr. Build. Mater.*, 2021, **310**, p 125291. <https://doi.org/10.1016/j.conbuildmat.2021.125291>
54. V. Nguyen-Van, N.K. Choudhry, B. Panda et al., Performance of concrete beam reinforced with 3D printed Bioinspired primitive scaffold subjected to three-point bending, *Autom. Constr.*, 2022, **134**, p 104060
55. H.Y. Sarvestani, A.H. Akbarzadeh, H. Niknam, and K. Hermenean, 3D printed architected polymeric sandwich panels: energy absorption and structural performance, *Compos. Struct.*, 2018, **200**, p 886–909
56. S. Hou, T. Li, Z. Jia, and L. Wang, Mechanical properties of sandwich composites with 3d-printed auxetic and non-auxetic lattice cores under low velocity impact, *Mater. Des.*, 2018, **160**, p 1305–1321
57. D. Xiao, X. Chen, Y. Li et al., The structure response of sandwich beams with metallic auxetic honeycomb cores under localized impulsive loading-experiments and finite element analysis, *Mater. Des.*, 2019, **176**, p 107840
58. H. Jiang, H. Ziegler, Z. Zhang et al., Bending behavior of 3D printed mechanically robust tubular lattice metamaterials, *Addit. Manuf.*, 2021, **50**, p 102565. <https://doi.org/10.1016/j.addma.2021.102565>
59. N.K. Choudhry, S.R. Bankar, B. Panda, and H. Singh, Experimental and numerical analysis of the bending behavior of 3D printed modified auxetic sandwich structures, *Mater. Today Proc.*, 2021, **56**, p 1356–1363
60. A. Beharic, R.R. Egui, and L. Yang, Drop-weight impact characteristics of additively manufactured sandwich structures with different cellular designs, *Mater. Des.*, 2018, **145**, p 122–134
61. H.L. Tan, Z.C. He, E. Li et al., Energy absorption characteristics of three-layered sandwich panels with graded re-entrant hierarchical honeycombs cores, *Aerosp. Sci. Technol.*, 2020 <https://doi.org/10.1016/j.ast.2020.106073>
62. Z.-D. Ma, H. Bian, C. Sun, G.M. Hulbert, K. Bishnoi, F. Rostam-Abadi, Functionally-graded NPR (negative Poisson's ratio) material for a blast-protective deflector. in NDIA Ground Vehicle Systems Engineering and Technology Symposium Modeling & Simulation, Testing and Validation (MSTV) Mini-Symposium, Dearborn, Michigan, 2010
63. L. Ji, W. Hu, R. Tao et al., Compression behavior of the 4D printed reentrant honeycomb: experiment and finite element analysis, *Smart Mater. Struct.*, 2020 <https://doi.org/10.1088/1361-665X/ababe4>
64. M. Wagner, T. Chen, and K. Shea, Large shape transforming 4D auxetic structures, *3D Print Addit. Manuf.*, 2017, **4**, p 133–142
65. F. Momeni, X. Liu, J. Ni et al., A review of 4D printing, *Mater. Des.*, 2017, **122**, p 42–79
66. M.H. Yousuf, W. Abuzaid, and M. Alkhader, 4D printed auxetic structures with tunable mechanical properties, *Addit. Manuf.*, 2020, **35**, p 101364. <https://doi.org/10.1016/j.addma.2020.101364>

67. T.R. Giri and R.W. Mailen, Thermomechanical behavior of polymeric periodic structures, *Addit. Manuf.*, 2022, **49**, p 102512. <https://doi.org/10.1016/j.addma.2021.102512>
68. K. Liu, L. Han, W. Hu et al., 4D printed zero Poisson's ratio metamaterial with switching function of mechanical and vibration isolation performance, *Mater. Des.*, 2020 <https://doi.org/10.1016/j.matdes.2020.109153>
69. M. Bodaghi, A.R. Damanpack, and W.H. Liao, Adaptive metamaterials by functionally graded 4D printing, *Mater. Des.*, 2017, **135**, p 26–36
70. M. Bodaghi, A.R. Damanpack, and W.H. Liao, Triple shape memory polymers by 4D printing, *Smart Mater. Struct.*, 2018, **27**, p 65010
71. M. Bodaghi and W.H. Liao, 4D printed tunable mechanical metamaterials with shape memory operations, *Smart Mater. Struct.*, 2019, **28**, p 45019. <https://doi.org/10.1088/1361-665X/ab0b6b>
72. J. Fish, *Practical Multiscaleing*, John Wiley & Sons, Hoboken, 2013
73. R.R. Madke and R. Chowdhury, A multiscale continuum model for inelastic behavior of woven composite, *Compos. Struct.*, 2019, **226**, p 111267
74. M.H. Fu, O.T. Xu, L.L. Hu, and T.X. Yu, Nonlinear shear modulus of re-entrant hexagonal honeycombs under large deformation, *Int. J. Solids Struct.*, 2016, **80**, p 284–296
75. J. Zhang, G. Lu, D. Ruan, and Z. Wang, Tensile behavior of an auxetic structure: analytical modeling and finite element analysis, *Int. J. Mech. Sci.*, 2018, **136**, p 143–154
76. J. Dirrenberger, S. Forest, and D. Jeulin, Effective elastic properties of auxetic microstructures: anisotropy and structural applications, *Int. J. Mech. Mater. Des.*, 2013, **9**, p 21–33
77. J. Dirrenberger, S. Forest, and D. Jeulin, Elastoplasticity of auxetic materials, *Comput. Mater. Sci.*, 2012, **64**, p 57–61
78. C. Lira, P. Innocenti, and F. Scarpa, Transverse elastic shear of auxetic multi re-entrant honeycombs, *Compos. Struct.*, 2009, **90**, p 314–322
79. H. Wan, H. Ohtaki, S. Kotosaka, and G. Hu, A study of negative Poisson's ratios in auxetic honeycombs based on a large deflection model, *Eur. J. Mech.*, 2004, **23**, p 95–106
80. O. Levy, S. Krylov, and I. Goldfarb, Design considerations for negative Poisson ratio structures under large deflection for MEMS applications, *Smart Mater. Struct.*, 2006, **15**, p 1459
81. S. Gonella and M. Ruzzene, Homogenization and equivalent in-plane properties of two-dimensional periodic lattices, *Int. J. Solids Struct.*, 2008, **45**, p 2897–2915
82. N. Chan and K.E. Evans, Microscopic examination of the microstructure and deformation of conventional and auxetic foams, *J. Mater. Sci.*, 1997, **32**, p 5725–5736
83. Z.-X. Lu, Q. Liu, and Z.-Y. Yang, Predictions of Young's modulus and negative Poisson's ratio of auxetic foams, *Phys. Status solidi*, 2011, **248**, p 167–174
84. B.B. Babamiri, H. Askari, and K. Hazeli, Deformation mechanisms and post-yielding behavior of additively manufactured lattice structures, *Mater. Des.*, 2020, **188**, p 108443
85. I. Schmidt and N.A. Fleck, Ductile fracture of two-dimensional cellular structures—dedicated to Prof. Dr.-Ing. D. Gross on the occasion of his 60th birthday, *Int. J. Fract.*, 2001, **111**, p 327–342
86. N. Kumar, B. Panda, and S. Kumar, Thin-Walled Structures Enhanced energy absorption performance of 3D printed 2D auxetic lattices, *Thin-Walled Struct.*, 2023, **186**, p 110650. <https://doi.org/10.1016/j.tws.2023.110650>
87. Manual ASU (2014) The Abaqus Software is a product of Dassault Systèmes Simulia Corp. Provid RI, USA Dassault Systèmes, Version 6
88. J. Ruzicka, M. Spaniel, A. Prantl et al., Identification of ductile damage parameters in the ABAQUS, *Bull. Appl. Mech.*, 2012, **8**, p 89–92
89. J. Kramberger, B. Nečemer, and S. Glodež, Assessing the cracking behavior of auxetic cellular structures by using both a numerical and an experimental approach, *Theor. Appl. Fract. Mech.*, 2019, **101**, p 17–24
90. H.J. Böhm, A short introduction to continuum micromechanics. In *Mechanics of Microstructured Materials* (Springer Vienna, 2004), pp. 1–40. [https://doi.org/10.1007/978-3-7091-2776-6\\_1](https://doi.org/10.1007/978-3-7091-2776-6_1)
91. A. Anthoine, Derivation of the in-plane elastic characteristics of masonry through homogenization theory, *Int. J. Solids Struct.*, 1995, **32**, p 137–163
92. Y. Guo, J. Zhang, L. Chen et al., Deformation behaviors and energy absorption of auxetic lattice cylindrical structures under axial crushing load, *Aerosp. Sci. Technol.*, 2020 <https://doi.org/10.1016/j.ast.2019.105662>
93. L.L. Hu, Z.R. Luo, and Q.Y. Yin, Negative Poisson's ratio effect of re-entrant anti-trichiral honeycombs under large deformation, *Thin-Walled Struct.*, 2019, **141**, p 283–292. <https://doi.org/10.1016/j.tws.2019.04.032>
94. W. Zhang, S. Zhao, R. Sun et al., In-plane mechanical behavior of a new star-re-entrant hierarchical metamaterial, *Polymers (Basel)*, 2019 <https://doi.org/10.3390/polym11071132>
95. X. Zhao, Q. Gao, L. Wang et al., Dynamic crushing of double-arrowed auxetic structure under impact loading, *Mater. Des.*, 2018, **160**, p 527–537. <https://doi.org/10.1016/j.matdes.2018.09.041>
96. CORONAEdgewise compression of novel hexagonal hierarchical and asymmetric unit cells honeycomb metamaterials \_ Elsevier Enhanced Reader (1).pdf
97. H. Wang, Z. Lu, Z. Yang, and X. Li, A novel re-entrant auxetic honeycomb with enhanced in-plane impact resistance, *Compos. Struct.*, 2019, **208**, p 758–770. <https://doi.org/10.1016/j.compstruct.2018.10.024>
98. M. Shokri Rad, H. Hatami, R. Alipouri et al., Determination of energy absorption in different cellular auxetic structures, *Mech. Ind.*, 2019, **20**, p 15–20. <https://doi.org/10.1051/meca/2019019>
99. M.H. Luxner, J. Stampfl, and H.E. Pettermann, Finite element modeling concepts and linear analyses of 3D regular open cell structures, *J. Mater. Sci.*, 2005, **40**, p 5859–5866
100. M.F. Guo, H. Yang, and L. Ma, Design and characterization of 3D AuxHex lattice structures, *Int. J. Mech. Sci.*, 2020 <https://doi.org/10.1016/j.ijmecsci.2020.105700>
101. S.C. Daminabo, S. Goel, S.A. Grammatikos et al., Fused deposition modeling-based additive manufacturing (3D printing): techniques for polymer material systems, *Mater. Today Chem.*, 2020, **16**, p 100248
102. J.U. Surjadi, L. Gao, H. Du et al., Mechanical metamaterials and their engineering applications, *Adv. Eng. Mater.*, 2019, **21**, p 1800864
103. F. Sharma and U.S. Dixit, sustainability analysis of fused deposition modelling process, *Fused Depos. Model. Based 3D Print.*, 2021 [https://doi.org/10.1007/978-3-030-68024-4\\_13](https://doi.org/10.1007/978-3-030-68024-4_13)
104. F. Sharma and U.S. Dixit, An analytical method for assessing the utility of additive manufacturing in an organization, *J. Inst. Eng. Ser. C*, 2021, **102**, p 41–50
105. X. Li, Z. Lu, Z. Yang et al., Yield surfaces of periodic honeycombs with tunable Poisson's ratio, *Int. J. Mech. Sci.*, 2018, **141**, p 290–302. <https://doi.org/10.1016/j.ijmecsci.2018.04.005>
106. K. Wang, Y.-H. Chang, Y. Chen et al., Designable dual-material auxetic metamaterials using three-dimensional printing, *Mater. Des.*, 2015, **67**, p 159–164
107. W. Wu, D. Qi, W. Hu et al., Synchrotron X-ray micro-computed tomography imaging of 3D re-entrant micro lattice during in situ micro compression experimental process, *Mater. Des.*, 2020, **192**, p 108743
108. H. Yang and L. Ma, Design and characterization of axisymmetric auxetic metamaterials, *Compos. Struct.*, 2020, **249**, p 112560
109. X. Li, L. Gao, W. Zhou et al., Novel 2D metamaterials with negative Poisson's ratio and negative thermal expansion, *Extrem. Mech. Lett.*, 2019, **30**, p 100498
110. K. Essassi, J. Rebiere, A. El Mahi et al., Experimental and analytical investigation of the bending behaviour of 3D-printed bio-based sandwich structures composites with auxetic core under cyclic fatigue tests, *Compos. Part A Appl. Sci. Manuf.*, 2020, **131**, p 105775
111. B. Ling, K. Wei, Z. Wang et al., Experimentally program large magnitude of Poisson's ratio in additively manufactured mechanical metamaterials, *Int. J. Mech. Sci.*, 2020, **173**, p 105466
112. H.Y. Sarvestani, A.H. Akbarzadeh, A. Mirbolghasemi, and K. Hermenean, 3D printed meta-sandwich structures: failure mechanism, energy absorption and multi-hit capability, *Mater. Des.*, 2018, **160**, p 179–193
113. V.A. Lvov, F.S. Senatov, A.M. Korsunsky, and A.I. Salimon, Design and mechanical properties of 3D-printed auxetic honeycomb structure, *Mater. Today Commun.*, 2020, **24**, p 101173
114. S. Jeong and H.H. Yoo, Shape optimization of bowtie-shaped auxetic structures using beam theory, *Compos. Struct.*, 2019, **224**, p 111020
115. L. Geng, W. Wu, L. Sun, and D. Fang, Damage characterizations and simulation of selective laser melting fabricated 3D re-entrant lattices

- based on in-situ CT testing and geometric reconstruction, *Int. J. Mech. Sci.*, 2019, **157**, p 231–242
116. M. Ye, L. Gao, and H. Li, A design framework for gradually stiffer mechanical metamaterial induced by negative Poisson's ratio property, *Mater. Des.*, 2020, **192**, p 108751
  117. D. Xiao, Z. Dong, Y. Li et al., Compression behavior of the graded metallic auxetic reentrant honeycomb: experiment and finite element analysis, *Mater. Sci. Eng. A*, 2019, **758**, p 163–171. <https://doi.org/10.1016/j.msea.2019.04.116>
  118. H.M.A. Kolken, K. Lietaert, T. van der Sloten et al., Mechanical performance of auxetic meta-biomaterials, *J. Mech. Behav. Biomed. Mater.*, 2020, **104**, p 103658
  119. F. Sharma and U.S. Dixit, Fuzzy set based cost model of additive manufacturing with specific example of selective laser sintering, *J. Mech. Sci. Technol.*, 2019, **33**, p 4439–4449
  120. H. Yang, B. Wang, and L. Ma, Mechanical properties of 3D double-U auxetic structures, *Int. J. Solids Struct.*, 2019, **180**, p 13–29
  121. S. Li, H. Hassanin, M.M. Attallah et al., The development of TiNi-based negative Poisson's ratio structure using selective laser melting, *Acta Mater.*, 2016, **105**, p 75–83
  122. L. Yang, O. Harrysson, H. West, and D. Cormier, Mechanical properties of 3D re-entrant honeycomb auxetic structures realized via additive manufacturing, *Int. J. Solids Struct.*, 2015, **69**, p 475–490
  123. T.D. Ngo, A. Kashani, G. Imbalzano et al., Additive manufacturing (3D printing): a review of materials, methods, applications and challenges, *Compos. Part B Eng.*, 2018, **143**, p 172–196
  124. M. Kaur, T.G. Yun, S.M. Han et al., 3D printed stretching-dominated micro-trusses, *Mater. Des.*, 2017, **134**, p 272–280
  125. C.K. Chua, C.H. Wong, and W.Y. Yeong, *Standards, Quality Control, and Measurement Sciences in 3D Printing and Additive Manufacturing*, Academic Press, London, 2017
  126. I. Zein, D.W. Huttmacher, K.C. Tan, and S.H. Teoh, Fused deposition modeling of novel scaffold architectures for tissue engineering applications, *Biomaterials*, 2002, **23**, p 1169–1185
  127. M.R.K. Ravari, M. Kadkhodaei, M. Badrossamay, and R. Rezaei, Numerical investigation on mechanical properties of cellular lattice structures fabricated by fused deposition modeling, *Int. J. Mech. Sci.*, 2014, **88**, p 154–161
  128. M.S. Islam and P. Prabhakar, Interlaminar strengthening of multidirectional laminates using polymer additive manufacturing, *Mater. Des.*, 2017, **133**, p 332–339
  129. R. Johnston and Z. Kazancı, Analysis of additively manufactured (3D printed) dual-material auxetic structures under compression, *Addit. Manuf.*, 2021, **38**, p 101783. <https://doi.org/10.1016/j.addma.2020.101783>
  130. F. Usta, F. Scarpa, H.S. Türkmen et al., Multiphase lattice metamaterials with enhanced mechanical performance, *Smart Mater. Struct.*, 2020 <https://doi.org/10.1088/1361-665x/abd15d>
  131. L.R. Lopes, A.F. Silva, and O.S. Carneiro, Multi-material 3D printing: The relevance of materials affinity on the boundary interface performance, *Addit. Manuf.*, 2018, **23**, p 45–52. <https://doi.org/10.1016/j.addma.2018.06.027>
  132. G. Imbalzano, S. Linforth, T.D. Ngo et al., Blast resistance of auxetic and honeycomb sandwich panels: comparisons and parametric designs, *Compos. Struct.*, 2018, **183**, p 242–261
  133. G. Imbalzano, P. Tran, T.D. Ngo, and P.V.S. Lee, A numerical study of auxetic composite panels under blast loadings, *Compos. Struct.*, 2016, **135**, p 339–352
  134. G. Imbalzano, P. Tran, T.D. Ngo, and P.V.S. Lee, Three-dimensional modelling of auxetic sandwich panels for localised impact resistance, *J. Sandw. Struct. Mater.*, 2017, **19**, p 291–316
  135. Y. Zhao, Q. Zhang, Y. Li et al., Theoretical, emulation and experimental analysis on auxetic re-entrant octagonal honeycombs and its applications on pedestrian protection of engine hood, *Compos. Struct.*, 2021, **260**, p 113534. <https://doi.org/10.1016/j.compstruct.2020.113534>
  136. V. Amaya-Amaya, M. de Icaza-Herrera, A.L. Martínez-Hernández et al., Experimental approximation of the sound absorption coefficient ( $\infty$ ) for 3D printed reentrant auxetic structures of poly lactic acid reinforced with chicken keratin materials, *Mater. Lett.*, 2021 <https://doi.org/10.1016/j.matlet.2020.128757>
  137. K.E. Evans and A. Alderson, Auxetic materials: functional materials and structures from lateral thinking!, *Adv. Mater.*, 2000, **12**, p 617–628
  138. Z. Wang and H. Hu, Auxetic materials and their potential applications in textiles, *Text. Res. J.*, 2014, **84**, p 1600–1611
  139. A. Boakye, Y. Chang, K.R. Rafiu, and P. Ma, Design and manufacture of knitted tubular fabric with auxetic effect, *J. Text. Inst.*, 2018, **109**, p 596–602
  140. X. Ren, J. Shen, P. Tran et al., Auxetic nail: design and experimental study, *Compos. Struct.*, 2018, **184**, p 288–298. <https://doi.org/10.1016/j.compstruct.2017.10.013>
  141. R.J. van Arkel, S. Ghouse, P.E. Milner, and J.R.T. Jeffers, Additive manufactured push-fit implant fixation with screw-strength pull out, *J. Orthop. Res.*, 2018, **36**, p 1508–1518
  142. C. Luo, C.Z. Han, X.Y. Zhang et al., Design, manufacturing and applications of auxetic tubular structures: a review, *Thin-Walled Struct.*, 2021, **163**, p 107682
  143. M.S. Leung, K. Yick, Y. Sun et al., 3D printed auxetic heel pads for patients with diabetic mellitus, *Comput. Biol. Med.*, 2022, **146**, p 105582
  144. B. Taherkhani, M.B. Azizkhani, J. Kadkhodapour et al., Highly sensitive, piezoresistive, silicone/carbon fiber-based auxetic sensor for low strain values, *Sens. Actuators A Phys.*, 2020 <https://doi.org/10.1016/j.sna.2020.111939>
  145. Z. Wang, A. Zulifqar, and H. Hu, in *Auxetic composites in aerospace engineering*. Advanced composite materials for aerospace engineering. (Elsevier, 2016), pp. 213–240
  146. A. Haris, H.P. Lee, Finite element analysis and experimental investigation on the mechanical behaviours of multifunctional sandwich structures embedded with batteries. *Adv. Compos. Mater.* 2022, 31(1), pp. 86–101
  147. Y. Jiang, Z. Liu, N. Matsuhisa et al., Auxetic mechanical metamaterials to enhance sensitivity of stretchable strain sensors, *Adv. Mater.*, 2018, **30**, p 1706589
  148. T. Fey, F. Eichhorn, G. Han et al., Mechanical and electrical strain response of a piezoelectric auxetic PZT lattice structure, *Smart Mater. Struct.*, 2015, **25**, p 15017
  149. Y.-J. Lee, S.-M. Lim, S.-M. Yi et al., Auxetic elastomers: mechanically programmable meta-elastomers with an unusual Poisson's ratio overcome the gauge limit of a capacitive type strain sensor, *Extrem. Mech. Lett.*, 2019, **31**, p 100516
  150. S. Krödel, T. Delpero, A. Bergamini, P. Ermanni, D.M. Kochmann, 3D auxetic microlattices with independently controllable acoustic band gaps and quasi-static elastic moduli. *Adv. Funct. Mater.*, 2014, **16**(4) p 357–363. <https://doi.org/10.1002/adem.201300264>
  151. K. Mohapatra, D.P. Jena, Insertion loss of sonic crystal made with multi resonant shells. *Appl. Acoust.*, 2021, **171**, p 107676. <https://doi.org/10.1016/j.apacoust.2020.107676>
  152. K. Mohapatra, D.P. Jena, Acoustic attenuation of hybrid sonic crystal made with periodic cylindrical scatterers and porous panels. *Acoust. Aust.*, 2021, **49**(3), p 441–449. <https://doi.org/10.1007/s40857-021-00239-0>
  153. H. Hu, Z. Wang, and S. Liu, Development of auxetic fabrics using flat knitting technology, *Text. Res. J.*, 2011, **81**, p 1493–1502. <https://doi.org/10.1177/00405175111404594>
  154. H. Fan, A. Gao, G. Zhang et al., A facile strategy towards developing amphiphobic polysulfone membrane with double Re-entrant structure for membrane distillation, *J. Memb. Sci.*, 2020, **602**, p 117933

**Publisher's Note** Springer Nature remains neutral with regard to jurisdictional claims in published maps and institutional affiliations.

Springer Nature or its licensor (e.g. a society or other partner) holds exclusive rights to this article under a publishing agreement with the author(s) or other rightsholder(s); author self-archiving of the accepted manuscript version of this article is solely governed by the terms of such publishing agreement and applicable law.